contact mode. Topography measurements were conducted using standard probehand with an ACTA probe with tip length around 15 µm. XEP and XEI (Park Scientific Instruments) software packages were used for data acquisition and image processing respectively.

5.2.3. Determination of LCST Temperature by QCM-D Analysis

Quartz Crystal Microbalance with Dissipation (QCM-D)

The accurate determination for the LCST temperature is a key factor to better understand the effect of the cross-linker and the different copolymers in the thin film behavior. QCM-D (Model E1, Q-Sense) were used to evaluate the hydrogels, triplicate coated sensors were analyzed.

A QCM (Standford Research Systems 2004) consists of a thin quartz disc sandwiched between a pair of electrodes. Due to the piezoelectric properties of quartz, it is possible to excite the crystal to make it oscillate by applying an AC voltage across its electrodes. In general, the electrodes are made of gold, which can be coated with a wide range of different materials.

Figure 5.3. QCM-D image. Model E1 from Q-Sense

The resonance frequency (f) of the sensor depends on the total oscillating mass, including water coupled to the oscillation. When a thin film is attached to the sensor, the frequency decreases. If the film is thin and rigid the decrease in frequency is proportional to the mass of the film. In this way, QCMs operate as a very sensitive balance. The mass of the adhering layer

is calculated by using the Sauerbrey relation. Where C is a constant for the quartz crystal and n is the overtone number.

$$Am = \frac{C \cdot \Delta f}{n}$$

Equation 5.1.

In most situations the adsorbed film is not rigid and the Sauerbrey relation becomes invalid. A film that is "soft" (viscoelastic) will not fully couple to the oscillation of the crystal; hence the Sauerbrey relation will underestimate the mass at the surface. A soft film dampens the sensor's oscillation. The damping or energy dissipation (D) of the sensor's oscillation reveals the film's softness (viscoelasticity).

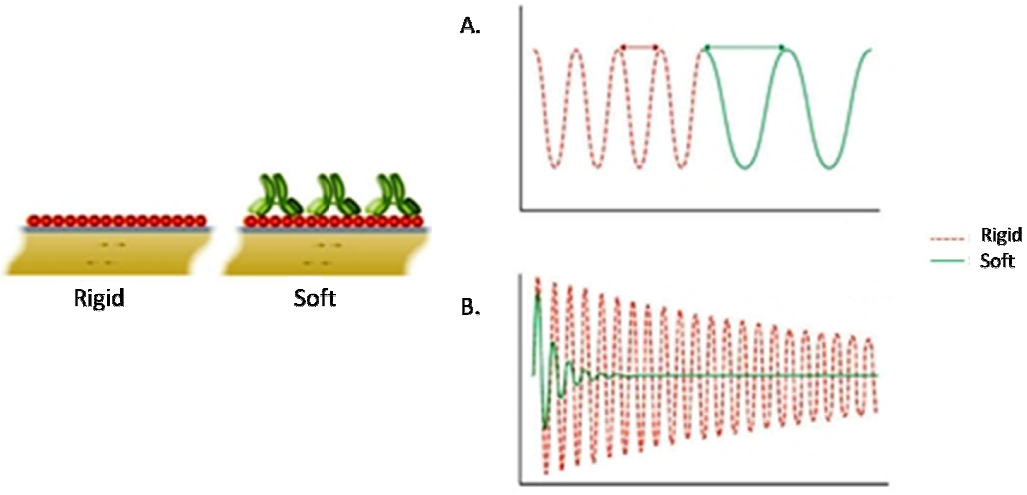

Figure 5.4. Real-time response of (A) frequency and (B) dissipation (QSense n.d.)

The modified sensors were placed in the flow cell with PBS buffer solution flowing at a rate of 50 µL/min. The chamber temperature was controlled with a Peltier heating element and was programmed to change the temperature at a rate of 1 ^{o}C/min, the films were assessed from 25

^{o}C to 55 ^{o}C and from 55 ^{o}C to 25 ^{o}C. During the first 5 min the temperature was maintained at 25 ^{o}C to assure that the film reached full equilibrium. This step is meant to avoid that the swelling process interfered in the LCST transition. Changes in both frequency and dissipation for harmonics of all orders (1, 3, 5, 7, 9, 11, and 13) were recorded to provide the whole information profile but only the data for the seventh harmonic is shown due to the good agreement between all of them. There is an inherent linear dependency of the QCM-D system on temperature (Ishida & Biggs 2007), so data obtained from blank crystal and from a film with no LCST transition were compared with thermo-responsive films to get the difference and obtain the LCST information.

5.2.4. Bacterial Adhesion, Proliferation and Detachment on Thermo-responsive Films

To test whether pNIPAAm films could achieve an improvement on the design of surfaces with bacterial resistivity, two different experimental series were performed. The experiments were designed to study bacterial adhesion on thermo-responsive hydrogels above and below their LCST. Both changes were studied, the first experimental setting monitored bacterial adhesion after transition of the hydrogel from its swollen to its collapsed state, thus bacterial cultures were first incubated at 37 ^{o}C and subsequently at 27 ^{o}C. In the second set of experiments, the influence of the hydrogel transition from collapsed to swollen state on bacterial adhesion was studied; thereby samples were first incubated at 27 ^{o}C and subsequently at 37 ^{o}C. Table 5.2. shows experimental conditions and Figure 5.5. represents the followed protocol schematically.

Table 5.2. Experimental conditions for all the samples incubated.
Samples with number 1 were first incubated at 37oC and then at 27oC. Samples with number 2, the incubated temperatures were swapped. Letter N was used for modified samples and B for unmodified.

Sample Name	1st Temp. (°C)	2nd Temp. (°C)
N1	37	27
PS1	37	27
N2	27	37
PS2	27	37

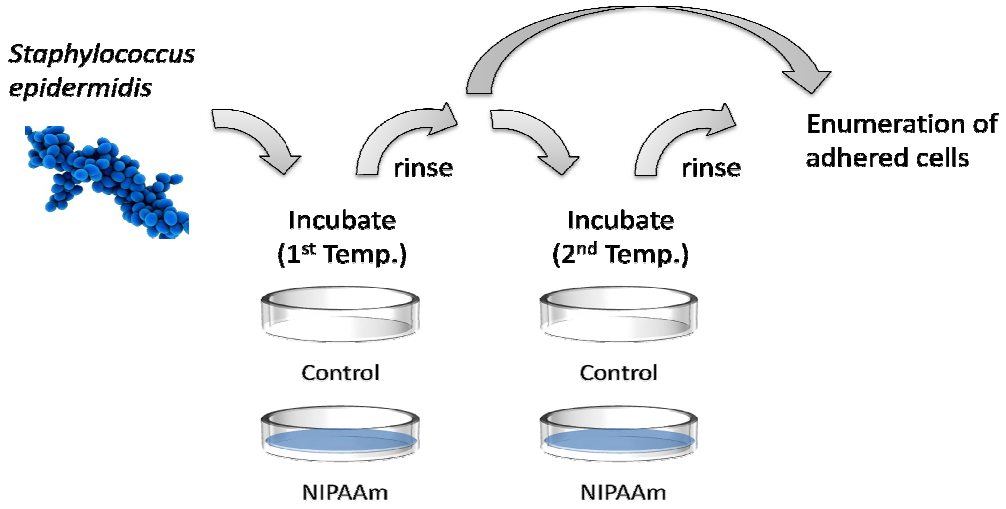

Figure 5.5. Schematic representation of the followed protocol to test pNIPAAm surfaces.

Staphylococcus epidermidis, gram-positive bacteria, was selected to perform bacterial adhesion studies. *S. epidermidis* is a bacterial strain that is known to form biofilms on devices placed within the body, such as catheter and prosthesis so it is a major concern in this application, therefore it is a relevant colonizing micro-organism for the scope of this thesis.

Prior to each experiment, a fresh bacterial suspension with an optical density at 600 nm (OD_{600}) between 0.2-0.3 was prepared from bacterial cells grown in nutrient TBS broth (Tryptic

soy broth, Merck) at 37 ^{o}C for 24 hours. The optical density for bacterial suspensions was adjusted on 6300 Spectrophotometer (Jenway).

Bacterial adhesion experiments were performed on tissue culture polystyrene plates (petri disches, Nunc), which were either used as received or modified with pNIPAAm hydrogel. Before use, petri dishes were washed extensively in 70% ethanol and sterile water then dried in sterile environment. Thermo-responsive samples, N samples, were introduced into the iCVD reactor to carry out the pNIPAAm thermo-responsive deposition, as described in 5.2.1. Bacterial cultures (2.5 mL) were added to modified and unmodified Petri dishes and incubated at either 37 ^{o}C (PS1 & N1) or 27 ^{o}C (PS2 & N2) for 3 hours. After incubation, the samples were washed three times with media and half of them were kept for bacterial quantification and, the rest were incubated at a different temperature, 27 ^{o}C (PS1 & N1) or 37 ^{o}C (PS2 & N2) for 1 hour. At the end of the second incubation time, the samples were rinsed three times with media and bacterial adhesion was quantified. Triplicates were performed for each incubation step in order to do statistical analysis of the results

To quantify the remaining adhered bacterial cells in each sample, 1.5 mL of PBS was added into the culture plates and cells were detached by sonication for 3 min in an ultrasonic bath (JP Selecta, 100 W). The supernatant was retired and the bacteria were pelleted by centrifugation (Sigma 1-14, at 1300 rpm , 5 min). Then 1.3 mL of supernatant was removed and bacteria were re-suspended by vortexing (Humblot et al. 2009). Appropriate serial dilutions were made and the samples were seeded onto agar plates. The plates were incubated for 24 hours at 37 ^{o}C and the number of colonies was counted.

Standard plate count method was used to determine adhered cells; each viable cell was separate from all others and developed into a single discrete colony (colony-forming units

CFUs). As the number of colonies gives the number of live cells that can grow under the incubation conditions, bacterial adhesion of the studied samples can be evaluated. The number of bacteria (CFU) per milliliter was calculated by dividing the number of colonies by dilution factor multiplied by the amount of specimen plated:

$$CFU = \frac{number\ of\ colonies}{dilution\ factor\ \times amount\ plated}$$

Equation 5.2.

5.2.5. Preparation of a Control Release System based on Thermo-responsive Films

In order to determine the capacity of NIPAAm thin film hydrogels to release Bacitracin, experiments were designed to study the microorganism alive on thermo-responsive hydrogels above their LCST, when the Bacitracin was released.

Bacitracin (Sigma Aldrich) was the chosen antibiotic due to its extensive use. This antibiotic is a common ingredient in skin antibiotic preparations and its action is on gram-positive bacteria. For the mentioned purpose, two surfaces were analyzed at 37 ^{o}C

Bacterial experiments were performed on tissue culture polystyrene plates (petri disches, Nunc), which were either used as received or modified with pNIPAAm hydrogel. Before use, petri dishes were washed extensively in 70% ethanol and sterile water then dried in sterile environment. Thermo-responsive samples, i.e. pNIPAAm samples, were introduced into the iCVD reactor to carry out the pNIPAAm thermo-responsive deposition, as described in 5.2.1.

Prior to bacterial inoculation, PS and pNIPAAm surfaces were loaded with Bacitracin (Sigma Aldrich, from *Bacillus licheniformis*, ≥50,000 U/g) (PS-B and NIPAAm-B). A solution of 1 mM was introduced into the petri dishes and the samples were cooled down to 10 ^{o}C for three hours, and then heated quickly to 37 ^{o}C, as it has been reported before (Leobandung et al. 2002). After this process, the samples were rinsed subsequently to wash the un-loaded Bacitracin. For the comparison purpose, PS and pNIPAAm hydrogel (PS-O and NIPAA-O) samples without embedded Bacitracin were used as a control.

Once all the surfaces were prepared, bacterial cultures (2.5 mL) were added to PS-O, NIPAAm-O (without Bacitracin), PS-B, and NIPAAm-B (with Bacitracin) petri dishes and incubated at 37 ^{o}C. The same fresh bacterial suspension from experiment 5.2.4. (OD_{600} = 0.2-0.3) was used to carry out this experiment. Table 5.3. shows the experimental modification for the different surfaces.

Table 5.3. Modifications applied to each surface to carry out the *in-vitro* experiments.

Sample Name	**iCVD modification**	**Drug delivery system**
PS-O	-	Control
PS-B	-	Bacitracin
NIPAAm-O	A1	Control
NIPAAm-B	A1	Bacitracin

To analyze the effect of the Bacitracin on the surfaces, supernatant was removed at 2, 4 and 24 hours and the number of bacteria was quantified by the standard plate count method (see 5.2.4.). After the supernatant was retired, bacteria was fully detached from the surfaces by vigorous pipetting (Räsänen 1981) for 2 minutes and incubated with new media until the next pre-determined period.

5.3. Results

In order to identify the LCST of the coatings and how it varies between them, four experimental settings were conducted. The first set of experiments was designed to investigate the NIPAAm's LCST and the effect of the cross-linker used during the deposition to obtain stable coatings in water (experimental series A). The rest of the experiments were designed to obtain a library of temperature responsive hydrogels with different LCST depending of the copolymer used during the deposition. Experimental series B and C resume the influence as a copolymer of DMAAm and AAc respectively. In experimental series D the main monomer, NIPAAm was substituted for DEAAm, and DMAAm was used as a co-monomer.

5.3.1. Surface Characterization of Thermo-responsive Hydrogels

Water Contact Angle

Thermo-responsive copolymerization via iCVD is achieved by flowing the monomers and the cross-linker into the reactor, as described earlier in 5.2.1. The monomers composition can be systematically modified by adjusting their relative flow-rates. The use of two different monomers and the degree of the cross-linker were analyzed to determine their influence on the hydrogels behavior. The changes in the hydrogels composition are clearly observed in the static water contact angle (WCA) measurements of the different polymers.

Figure 5.6. shows switchable surface properties imparted by tunable p(NIPAAm) copolymers. The experiments were done increasing the temperature from 25 ^{o}C (room temperature) to a temperature of 50 ^{o}C, above the LCST, to study the wettability changes before and after the phase-transition. The results confirm that thermo-responsive hydrogels have been synthesized

due to the influence of the temperature in the surface behavior. As the temperature was increased the hydrophobicity of the film was also increased, this wettability changes are caused by the phase transition, and the hydrogel was collapsing in water above a certain temperature.

Top images in Figure 5.6. shows the typical water contact angle of NIPAAm-co-EGDA deposited via iCVD. A1 sample (NIPAAm/EGDA, 90/10) presented a change in WCA measurement of 31^{o}, when the temperature of the hydrogel was increased from RT to 50 ^{o}C. Comparable results have been previously reported (Sun et al. 2004), which confirms that pNIPAAm was successfully deposited on the surfaces. Regarding B2 (NIPAAm/DMAAm/EGDA, 70/20/10) and C2 (NIPAAm/AAc/EGDA, 70/20/10) samples, NIPAAm was copolymerized with two different monomers, DMAAm and AAc respectively, whereas EGDA was maintained constant in order to maintain the same cross-linking density. When a drop of PBS solution was deposited on either B2 or C2 at room temperature, the resulting contact angle, 54^{o} and 51^{o} respectively, was lower, when compared to the NIPAAm sample A1, 71^{o}. These results indicate an increase in the hydrophilicity of B2 and C2 hydrogels, which is in good agreement with the expected results, since DMAAm and AAc are more hydrophilic than NIPAAm.

The same effect was also observed when contact angle were measured above the LCST. Warm PBS droplet was pulled to a 50 ^{o}C heated surfaces and the final WCA was decreased from the A1 hydrogel, the hydrophobic behavior that was achieved in the first case was reduced in the next cases due to the use of hydrophilic monomers, giving a WCA around 77^{o} and 71^{o} (DMAAm and AAc copolymers respectively).

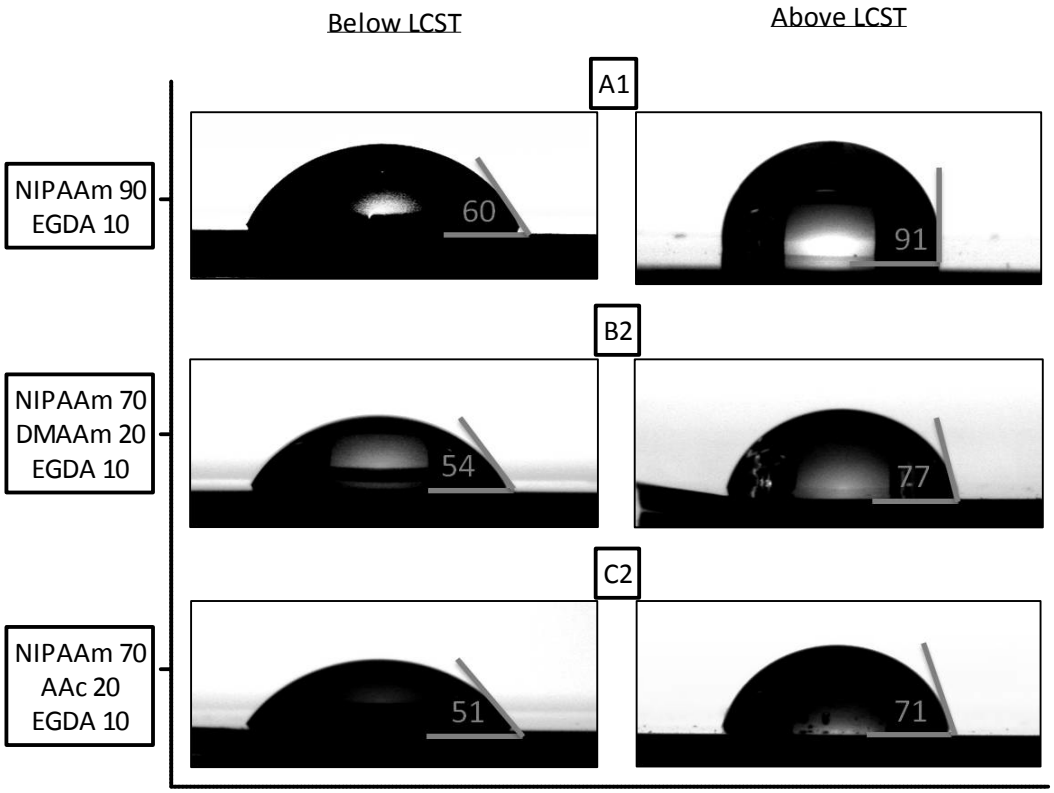

Figure 5.6. Static contact angles, below and above LCST, of different NIPAAm copolymers. A1 sample, NIPAAm-co-EGDA (top-centered), B2 sample, NIPAAm-co-DMAAm-co-EGDA (middle-centered) and C2, NIPAAm-co-AAc-co-EGDA (down-centered)

Although B2 and C2 surfaces also exhibited remarkable changes between the WCA below and above the LCST, differences between WCA values were significantly lower when compared to the sharp change around 30^{o} obtained for pNIPAAm samples. DMAAm and AAc hydrogel copolymers, B2 and C2, presented differences in WCA values of 23^{o} and 20^{o}, respectively, as shown in Figure 5.7.

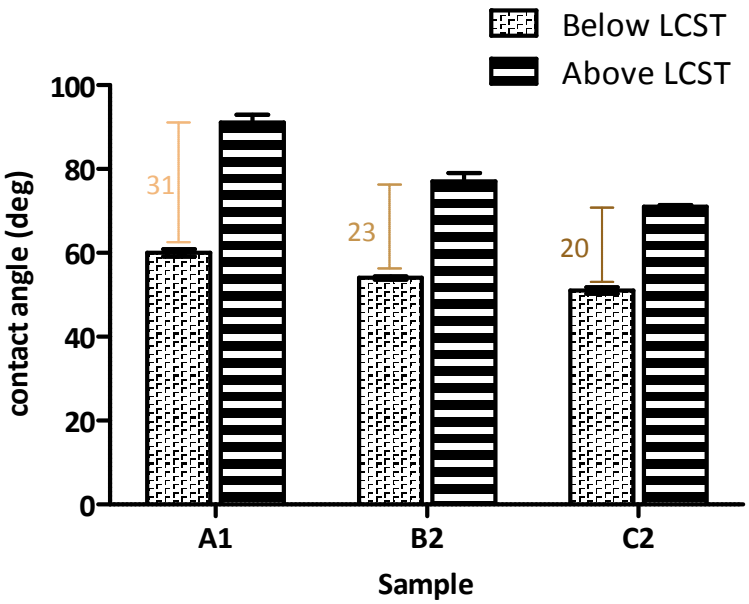

Figure 5.7. WCA representation below and above LCST for three samples.
A1 sample, NIPAAm-co-EGDA, B2 sample, NIPAAm-co-DMAAm-co-EGDA and C2, NIPAAm-co-AAc-co-EGDA.

In order to confirm that the hydrophilicity of the monomers plays an important role in the phase transition of the resulting thermo-responsive hydrogels, hydrogel A1 was compared with a hydrogel made with a more hydrophilic thermo-sensitive monomer, which was prepared with a more hydrophilic thermo-sensitive monomer. In this case, the ratio between the monomer and the cross-linker was maintained constant while the NIPAAm was substituted by DEAAm.

Figure 5.8. shows the dependence of the monomer on the contact angle, below and above the LCST. As it has been observed before, when a more hydrophilic monomer was used for the iCVD deposition, lower contact angle values were observed on the resulting surfaces both

before and after the phase-transition. DEAAm film exhibited a 26° change in WCA measurement, 5° less than NIPAAm film synthesized under the same conditions.

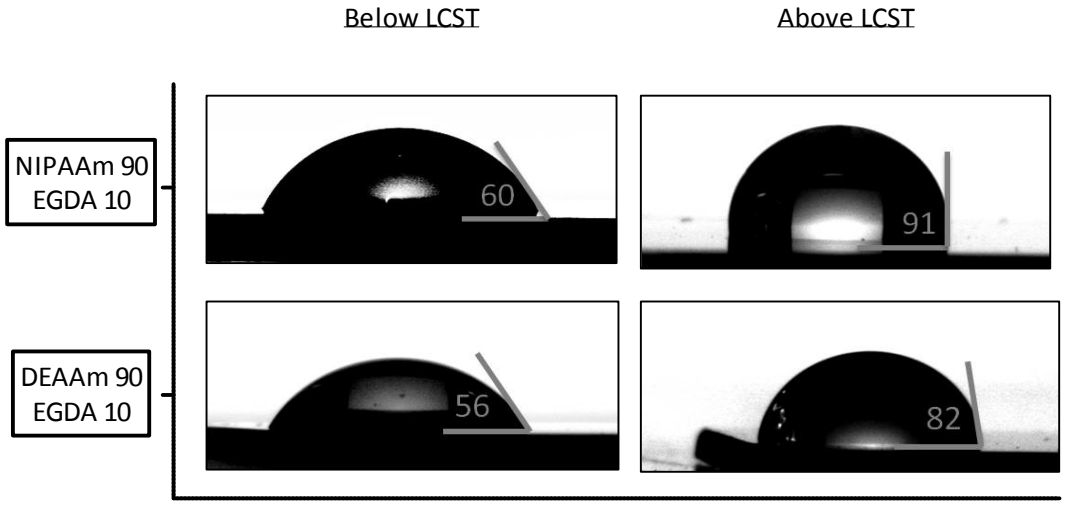

Figure 5.8. Static contact angles, below and above the LCST, of NIPAAm and DEAAm films. NIPAAm-co-EGDA (top-centered) and DEAAm-co-EGDA (down-centered)

Atomic Force Microscopy

Further characterization of the obtained co-polymers was performed by AFM to analyze and measure surface topography. NIPAAm copolymer surfaces used to determine WCA were analyzed. The study was carried out under dry mode at room temperature to better understand the hydrogel surface without water interactions.

Topography images (Figure 5.9) obtained from a 10 x 10 μm^2 area confirmed that the hydrogel surfaces were different in each case, as shown in Figure 5.9. As it has been determined, the presence of another type of acrylamide or the amount of acrylic acid increases the roughness,

which might explained the changes in the wettability of NIPAAm hydrogels, as can be observed in Figure 5.7.

Typical smooth pNIPAAm hydrogel with a 10% of cross-linker was observed, having a root-mean-square (rms) roughness of 1.5 nm on the area selected (10x10 μm^2). Although homogeneous surface was achieved, occasional isolated features were observed indicating different areas. This might be explained by formation of hydrophilic domains in the matrix structure as revealed by AFM imaging in Figure 5.10.

Figure 5.9 and Figure 5.10 explores the changes in B2 and C2 hydrogels, in order to compare with the pure NIPAAm (A1 sample). The results show an increase of the roughness as the hydrophilicity was increased. As it has been discussed, the incorporation of this kind of copolymers increased the formation of hydrophilic domains resulting in a rougher surface. The number of isolated features created in C2 hydrogel made a huge difference between A1 and B2 film.

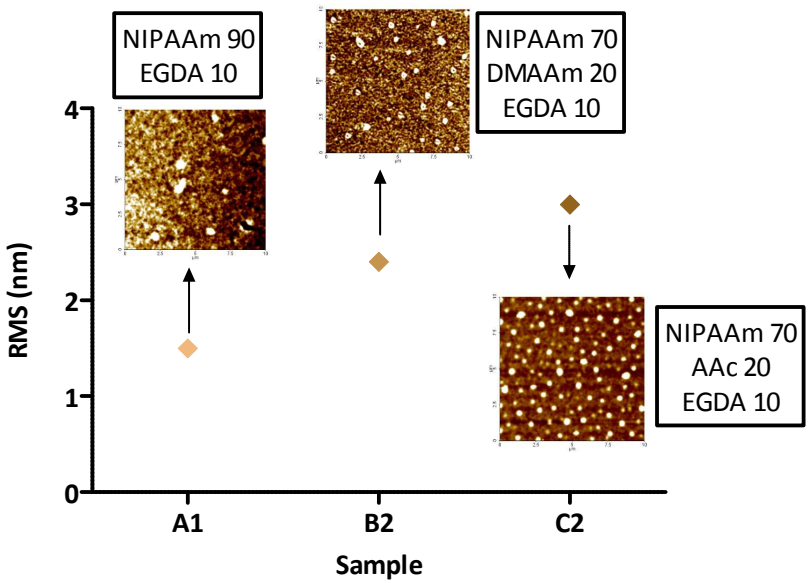

Figure 5.9. AFM images of the NIPAAm copolymers surfaces together with their roughness.

A1 sample, NIPAAm-co-EGDA, B2 sample, NIPAAm-co-DMAAm-co-EGDA and C2, NIPAAm-co-AAc-co-EGDA.

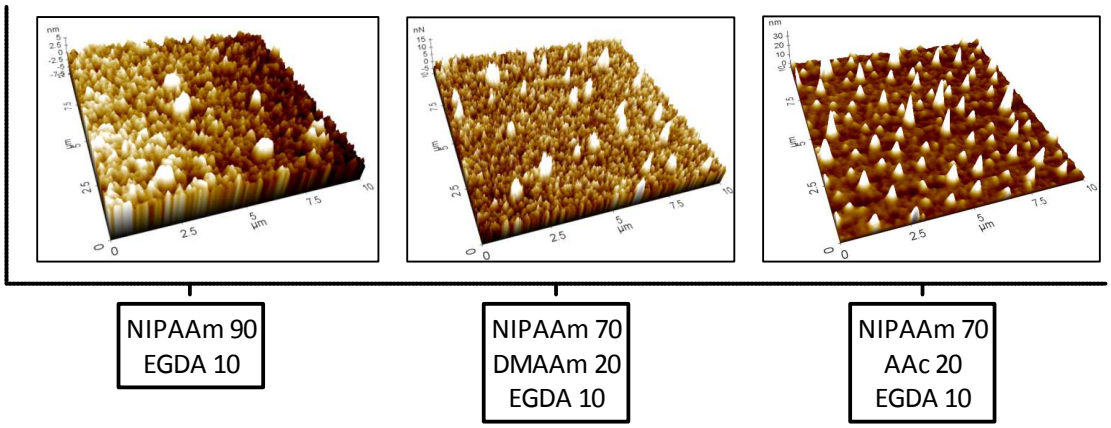

Figure 5.10. 3D AFM images of NIPAAm hydrogels.

A1 sample, NIPAAm-co-EGDA, B2 sample, NIPAAm-co-DMAAm-co-EGDA and C2, NIPAAm-co-AAc-co-EGDA.

5.3.2. Determination of the LCST Temperature via QCM-D Analysis

As it has been already described, the hydrogel polymer chains collapse upon heating due to hydrophobic interactions, resulting in a change of the mass and the viscoelasticity of the hydrogel that can be monitored by the frequency and dissipation variation using QCM-D analysis.

In order to assure the use of this system to detect the LCST, the QCM-D analysis of a non thermo-responsive hydrogel and a pNIPAAm hydrogel were compared. Both hydrogels were NIPAAm based polymers but with different NIPAAm/EGDA flow-rates. In the first case the NIPAAm flow was 10% (N10) and in the other was 90% (N90).

Figure 5.11. shows the linear dependency of the QCM-D on temperature. The fact that the frequency of the N10 hydrogel follows the same trend as the temperature indicates that the polymer did not suffer any mass changes during the temperature transition. As it has been mentioned before, there is an intrinsic dependence of the resonant frequency of a quartz crystal on temperature, thus a carefully control of the temperature effect must be done. The resonance frequency depends on temperature, pressure and bending stress. Temperature gradients causes internal stresses, which induced frequency variation even no mass change is achieved.

On the contrary, the frequency of the N90 hydrogel showed an inflection point that corresponds to the LCST temperature. The slope decreased after the LCST transition because the hydrogel behavior was clearly changing, since the thermo-responsive polymer collapsed and the mass decreased due to the NIPAAm dehydration.

Moreover, it was often observed that the frequency *vs*. temperature curve obtained going from T1 to T2 did not coincide with the one obtained immediately after going from T2 to T1. This effect might be caused by the low capacity of the peltier element to dissipate the heat (1 ^{o}C/min) from the cell when temperature was decreasing.

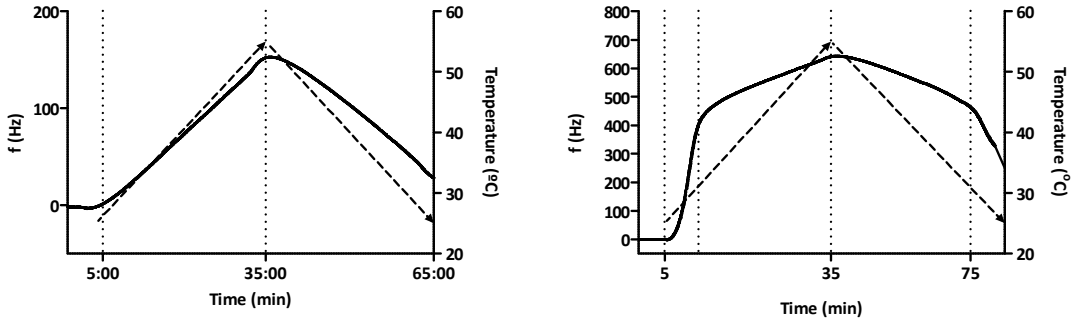

Figure 5.11. QCM-D graphs confirming the linear dependency of the f on temperature.
The dashed line indicates the temperature ramp. Frequency of QCM-D coated crystals sensors with a non thermo-responsive hydrogel (left) and one hydrogel that show the LCST transition.

QCM-D analysis can also provide information concerning the reversible transition that caused the temperature in the hydrogel. Figure 5.12. demonstrates that the hydrogel collapsed around 32 ^{o}C when the temperature was increased and the same change in the slope occured when the temperature was decreased, the hydrogel swelled once the temperature reached the LCST. The gradual variation in energy dissipation of the N90 layer as the temperature increased is shown in Figure 5.12.(b). Once the equilibrium was reached, the dissipation decreased indicating that the thin film was softer due to the swollen state of the hydrogel. After the LCST temperature, the dissipation slope changes because the hydrogel was collapsed and the film was in its rigid state.

(a) (b)

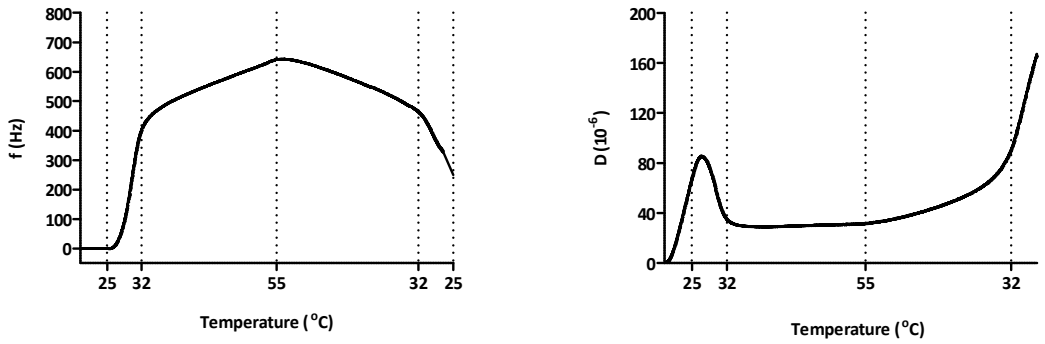

Figure 5.12. Representative results showing the (a) frequency and (b) dissipation for N90 hydrogel. The data was recorded for a temperature ramp from 25 °C to 55 °C and vice versa.

5.3.3. Development of a Library of Thermo-responsive Hydrogels

Due to the large amount of experiments that can be generated to have enough information to create a library, four different experiments were chosen. The study was carried out with the aim of comparing the thermo-sensitive behavior of bulk hydrogels previously prepared in our group with thermo-sensitive thin films (Garreta 2005). The possibility to obtain the same bulk hydrogel properties, but located within a thin film that can be deposited in almost every surface was the starting point for this work.

The principle idea was to analyze how the monomer's hydrophilicity, the ratio between the monomers and the ratio of the cross-linker could influence the LCST transition and the QCM-D studies. Experimental series A, B, C was design to obtain an LCST between 30-40 °C, NIPAAm was used as the main monomer because its phase-transition temperature in aqueous solution

is around 32 ^{o}C (Schild 1992). In experimental series D, NIPAAm was replaced by DEEAm as the main monomer to obtain an increase in the LCST temperature.

The first step was to demonstrate the possibility to achieve a NIPAAm thin film hydrogel via iCVD that could reproduce the LCST for bulk hydrogels. Three different ratios of NIPAAm and EGDA were compared to evaluate the influence of the cross-linker in the resulting films. Figure 5.13. shows the QCM-D analysis of the three different films. Results indicate that there was a relationship between the monomer/cross-linker ratio and the LCST, when the level of NIPAAm is lower the effect of the cross-linker is higher. A1 presented an LCST of 32 ^{o}C, the same temperature as bulk synthesized pNIPAAm, and the change in the slope is deeply marked by the phase-transition indicating that the hydrogel is collapsing. The same occurs in A2 films, where the variation is clearly observed, although the LCST temperature increased by 2 ^{o}C. When the level of EGDA was higher, as in A3 hydrogel, the frequency and dissipation changes, around 38 ^{c}C, were smoother meaning that the hydrogel dehydratation caused by transition from the swollen to the collapsed state was reduced. The cross-ling density controls the degree of hydratation of the films.

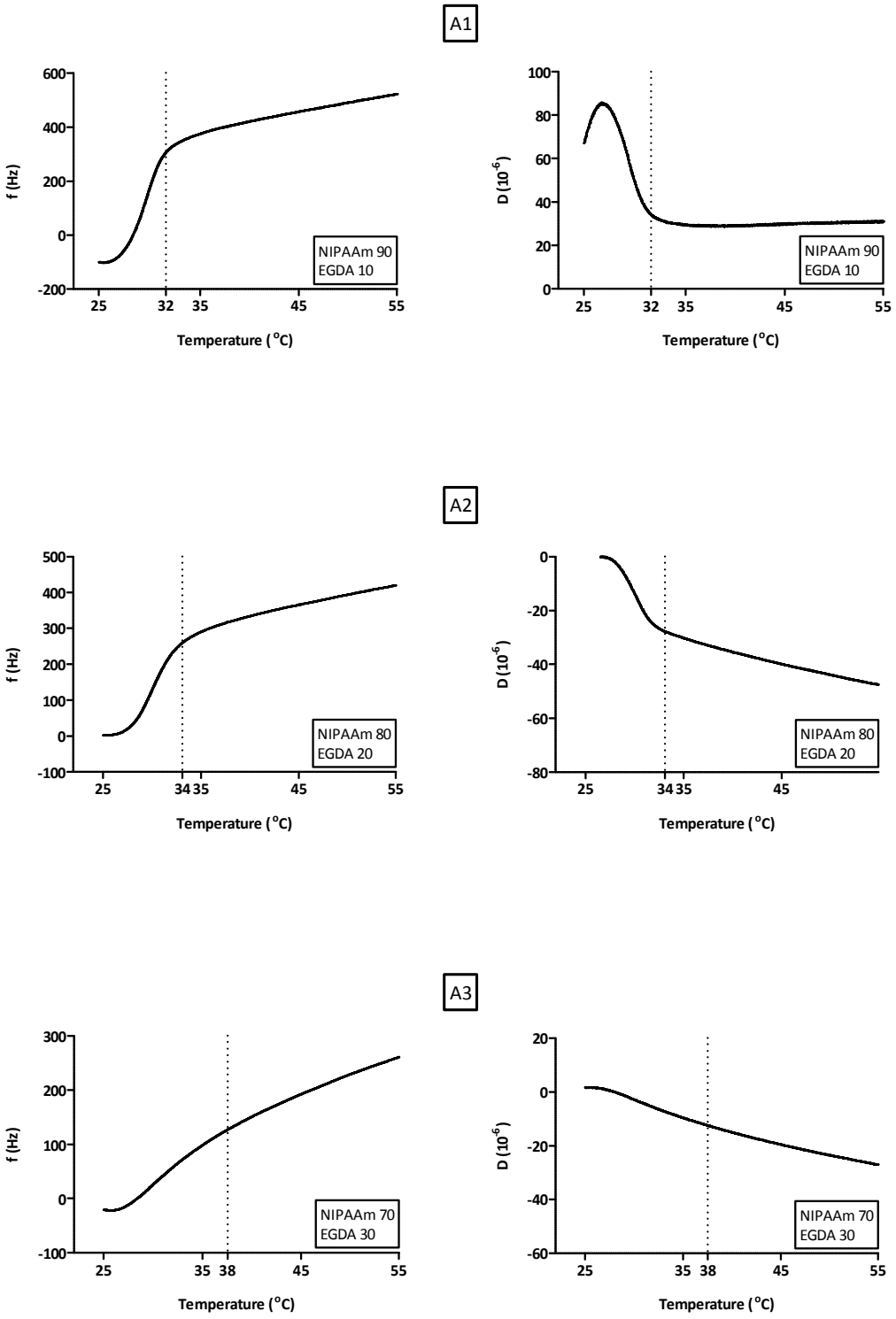

Figure 5.13. LCSTs corresponding to NIPAAm-co-EGDA thin films.

(A1) 90% of NIPAAm, (A2) 80% of NIPAAm and (A3) 70% of NIPAAm. The graph shows the three variations in EGDA ratio.

As it has been mentioned, the temperature range is mainly controlled by the NIPAAm. Nevertheless, the amount of cross-linker and the nature and ratio of the co-monomer, can be used to tune the LCST of the resulting films. The next step involved the assessment of the influence of two different co-monomers, DMAAm and AAc, and the ratios between NIPAAm and them. For this purpose, pNIPAAm hydrogels having varying concentrations of DMAAm or AAc were synthesized at a fixed cross-linker ratio of 10% and their thermosensitive behavior was assessed using QCM-D analysis.

Results for the hydrogels based on NIPAAm-co-DMAAm are shown in Figure 5.14. A trend toward higher LCST with increasing DMAAm was observed in the three experiments. An increase in LCST for copolymers of NIPAAm was typically attributed to an increase in the hydrophilicity of the copolymer (Schild 1992). The use of DMAAm increases the temperature transition from 4 ^{o}C to 8 ^{o}C, when compared to pNIPAAm hydrogels, as observed in experiments B1, B2 and B3 respectively. The higher temperature was achieved with a higher concentration of DMAAm. This result could be explained taking into account that the copolymer increases the hydrophilicity of the final thin film hydrogel, giving the capacity to shift the LCST of pNIPAAm-based hydrogel to higher temperatures.

The hydrogel B1, which has 90% of NIPAAm and 10% of DMAAm shows an abrupt LCST transition. The pronounced variation in the frequency slope can be explained by the loose of a considerable amount of water upon heating beyond the LCST. The high capacity of the hydrogel to swell makes a sharp and fast transition. This phenomenon was not observed in B2 and B3 films were the changes were less perceptible. This behavior was also observed in bulk-synthesized polymers having approximately the same co-monomer and is probably explained

by an increase in the hydrophilicity of the polymer network making the transition from fully hydrated to collapsed.

These results could also explain the difference between the sharp LCST transition in B1 film and the smooth transition in B2 and B3. The fact that B1 film was highly hydrated explains the abrupt transition from swollen to collapsed state; in addition the change in the dissipation slope means that temperature goes from a really soft material to a rigid state. The same process was observed in the rest of the experiments but the change is smoother due to the minor phase-transition.

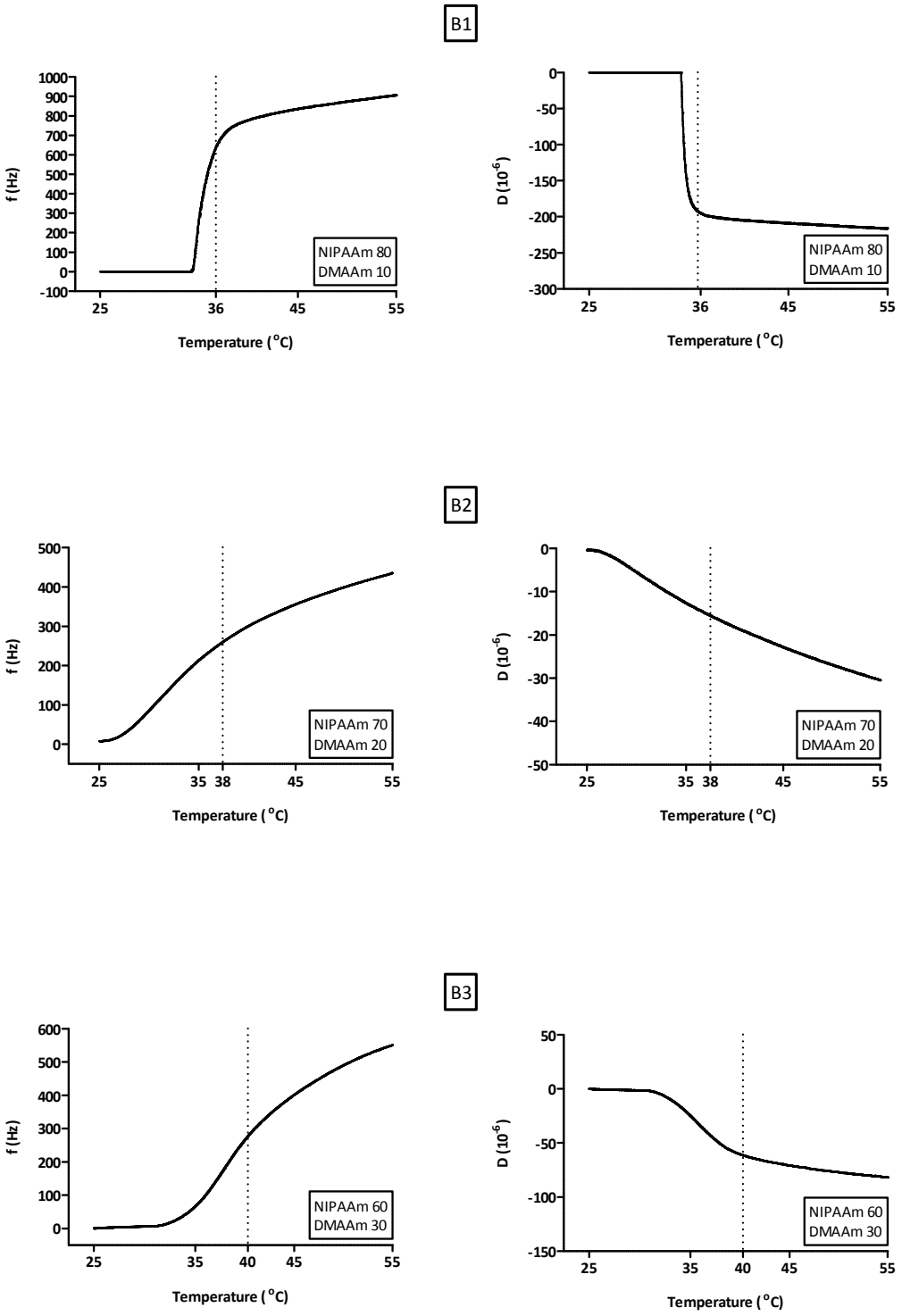

Figure 5.14. LCSTs corresponding to NIPAAm-co-DMAAm thin films.

(B1) 10% of DMAAm, (B2) 20% of DMAAm and (B3) 30% of DMAAm. The graph shows the three variations in NIPAAm/DMAAm ratios. The EGDA ratio was maintained constant at 10%.

As it has been observed in the case of NIPAAm/DMAAm co-polymers, addition of co-monomers can tune the LCST of the resulting hydrogel, therefore the next step was to analyze the influence of the co-monomer chemical nature. Acrylic acid was the co-monomer that was used to compare the influence of the co-monomer nature on the LCST. The target hydrogel was designed to have the same proportions as the DMAAm samples.The phase-transition of hydrogels made of NIPAAm/AAc co-polymers was monitored by QCM-D, as shown in Figure 5.15.

The first difference that can be extracted comparing Figure 5.14. and Figure 5.15 is that, in the case of using AAc as co-monomer, the transitions were smoother than in the case of DMAAm. In contrast to DMAAm, AAc-containing hydrogels did not show any sharp phase-transition, not even for hydrogels containing low ratios of AAc and high ratios of NIPAAm. As it has benn mentioned previously, the tuneable LCST and the behavior of the phase transition are determined by the hydrophilicity of the co-monomer. However, the pronounced hydrophilic character of AAc, which is conferred by the presence of a carboxylic acid group, results in the elimination of the hydrogel thermo-sensitivity.

Another noticeable difference was the changes observed in the QCM-D transition profile. When AAc co-monomer was present in the hydrogel, two transitions were observed during QCM-D analysis (Figure 5.15). This phenomenon has been known to be the result of an increase in the phase transition time. The first change in the slope, near the theoretical NIPAAm LCST temperature, is associated to the starting point of the phase-transition and once the hydrogel turned to a hydrophobic film and the chains were totally collapsed, the transition arrived to its end point, represented by the second change in the slope. Different behavior was

achieved whit NIPAAm-co-AAc hydrogels; and consequently phase transition rate could be tuned accordingly.

Nevertheless, these films exhibit a limit AAc concentration beyond which the hydrogels lose their thermo-sensitive capacity. In general, as the AAc ratio was increased, the transition period was also increased. However, for AAc ratios higher than 20% the resulting hydrogel coatings did not present any phase-transition during the temperature ramp

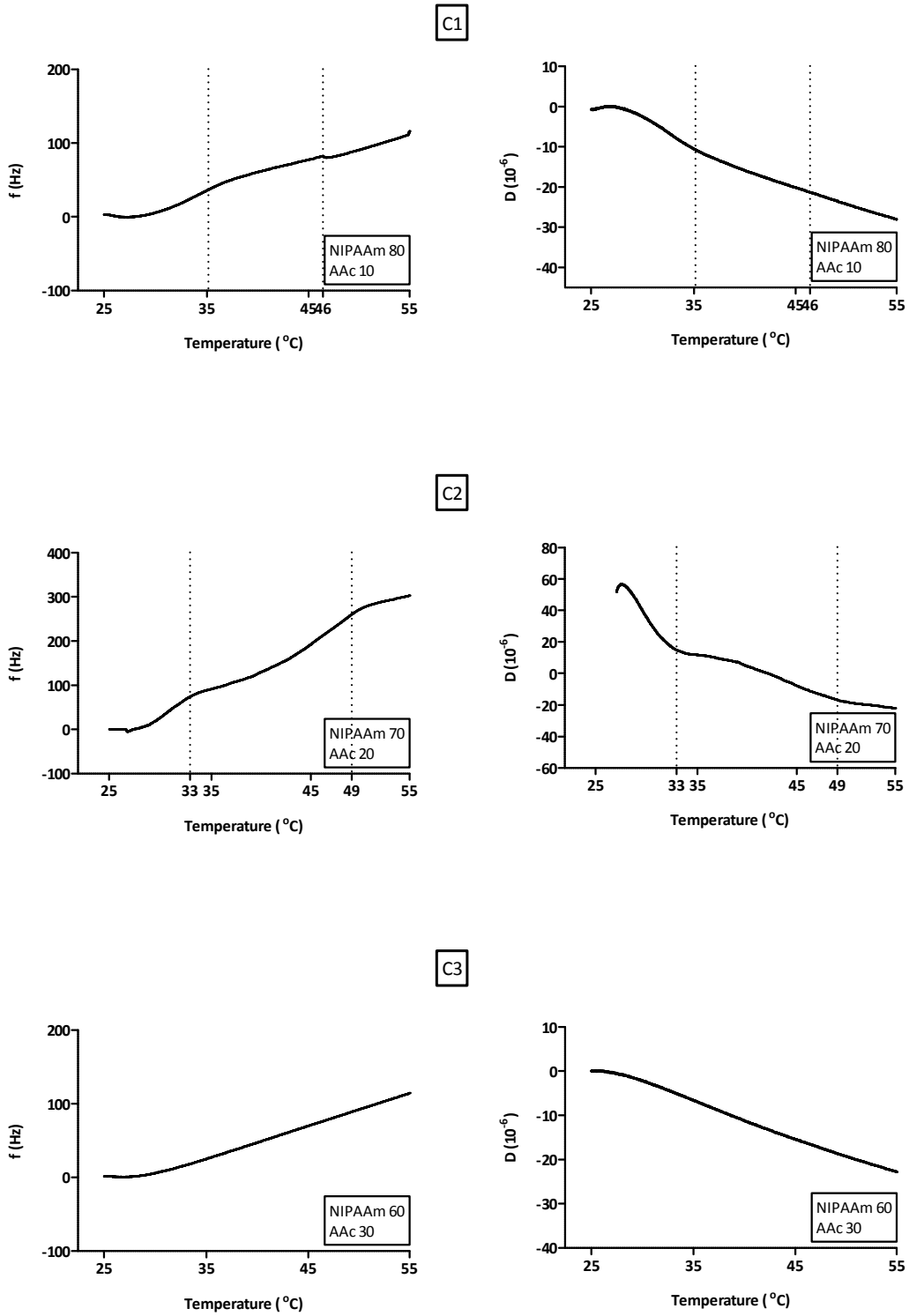

Figure 5.15. LCSTs corresponding to NIPAAm-co-AAc thin films.

(C1) 10% of AAc, (C2) 20% of AAc and (C3) 30% of AAc. The graph shows the three variations in NIPAAm/ AAc ratios. The EGDA ratio was maintained constant at 10%.

The last set of experiments regarding the development of the thermo-sensitive hydrogel library was designed to assess the influence of the main thermo-sensitive monomer. Therefore, the difference in thermo-sensitive behavior of hydrogels prepared from a different N-substituted acrylamide was studied. In bulk hydrogel synthesis, where DEAAm/DMAAm combinations were selected to obtain co-polymers with higher phase-transition temperatures, lower critical solution temperatures around 45 ^{o}C were obtained. Hydrogels synthesized from DEAAm alone were discarded, since the resulting LCSTs were above 70 ^{o}C, which is a value beyond the temperature range of the present study. Three different hydrogels D1 – D3 with DEAAm/DMAAm ratios varying from 90:10 to 60:30 were synthesized and their thermo-sensitive behavior was evaluated by QCM-D analysis, as shown in Figure 5.16.

Figure 5.16. shows the thermo-responsive behavior of D1 and D2 hydrogels determined by QCM-D analysis. D3 did not present any response against the temperature changes, indicating that the thermo-sensitive capacity was lost, similarly observed as in C3 hydrogel (NIPAAm/AAc/EGDA, 60/30/10).

As it can be observed, D1 and D2 presented a higher LCST temperature, when compared with B1 and B2 hydrogels, where the main monomer was NIPAAm and the co-monomer and the cross-linker were the same. An increase of 5 ^{o}C in the LCST was achieved when NIPAAm was substituted by DEAAm.

In contrast to NIPAAm-containing hydrogels, the phase transition of hydrogels prepared from DEAAm was less pronounced. The variation was smoother during the phase-transition and, only small changes in the slope were noticed in this case. Furthermore, D1 and D2 compositions presented similar thermo-sensitive behaviors and appoximately the same LCST temperatures were achieved, when the flow-rates between the monomers were different.

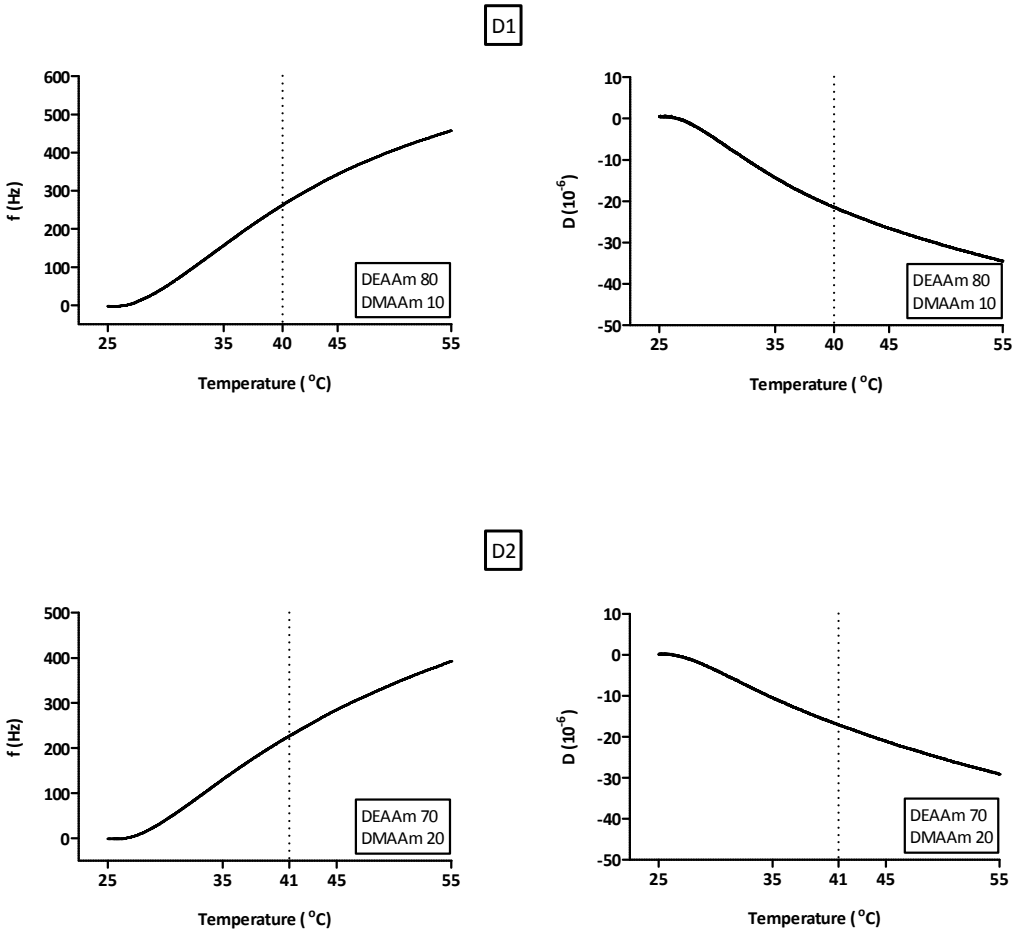

Figure 5.16.LCSTs corresponding to DEAAm-co-DMAAm thin films.

(D1) 80% of DEAAm and 10% of DMMAm, (D2) 70% of DEAAm and 20% of DMMAm. The graph shows both variations in DEAAm/DMAAm ratios. The EGDA ratio was maintained constant at 10%.

5.3.4. Monitoring of Bacterial Detachment upon Phase Transition

Once the characterization of thermo-responsive hydrogels was performed and their surface properties were analyzed, the next step was to test the potential of pNIPAAm hydrogels as anti-bioflim in a medium containing colonizing microorganisms.

Tissue culture polystyrene plates, either naïve or modified with pNIPAAm, were used to carry out this experiment. A1 sample (NIPAAm/EGDA - 90/10) was chosen to be deposited on petri dishes due to its sharp transition. This hydrogel presented both the largest WCA change and the highest hydrophobic surface above its LCST. The transition temperature achieved with this coating, around 32 ^{o}C, is ideal, because microorganisms remain alive both below and above the selected LCST.

Briefly, *S. Epidermidis* was seeded on either unmodified or pNIPAAm-modified petri dishes and incubated at either 37 ^{o}C (PS1 & N1) or 27 ^{o}C (PS2 & N2) for 3 hours. Samples were washed with media (TSB) and subsequently incubated at 27 ^{o}C (PS1 & N1) or 37 ^{o}C (PS2 & N2) for 1 hour. At the end of each incubation, adherent bacteria were quantified in order to compare the effect of the change on the hydrogel properties on bacterial attachment, as shown in Figure 5.17. Figure 5.17. shows the percentage of cell adhesion in both cases, the control (PS without further modification) and the NIPAAm hydrogel. During the first set of experiments, as the temperature was decreased, the hydrogel changed its phase from collapsed to swollen state.

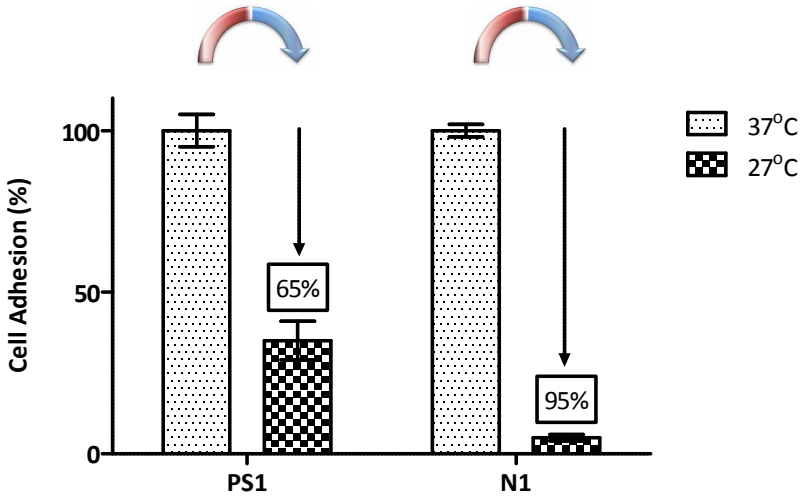

Figure 5.17. Percentage of cell adhesion when the temperature was decreased from 37 °C to 27 °C. Tissue cultured polystyrene plates, unmodified (PS1) or modified (N1) with pNIPAAm.

The number of adhered cells during the first incubation was considered the total amount of microorganism over the surfaces. After one hour at 27 °C, the percentage of bacterial cells that remained adhered was calculated respect to the total adhesion achieved during the first step. As it has been reported before, *Staphylococcus epidermis* showed a better and richer growth at 37 °C than at 27 °C, where the results showed that the adhered cells was four times smaller (Hola et al. 2006). Moreover, changes in the temperature could cause a decrease of metabolism of the cells, resulting in cell detachment, as can be observed for PS1 sample in Figure 5.17. In contrast, the detachment of bacteria for N1 could be explained, not only by the decrease of metabolism of cells caused by temperature, but more importantly, by changes in topography and wettability, as it can be observed in Figure 5.7. and Figure 5.9. In this situation, the adhered cells may easily fall apart and the detachment of large part of the adhered cells (95%) on N1 film was achieved due to the phase transition.

These results probably indicate that during phase-transition, the hydrogel surface, which served as substrate for bacteria, suffered a variation in its topography and wettability, resulting in increased cell detachment, when compared to PS samples.

In order to study phase transitions in both transitions (from 37 °C to 27 °C and *vice versa*), one changing from collapsed to swollen state and the other one from swollen to collapsed state, the incubation temperatures were swapped. In the second experimental series, the initial incubation temperature was set at 27 °C and cell detachment was assessed after incubation at 37 °C, as shown in Figure 5.18.

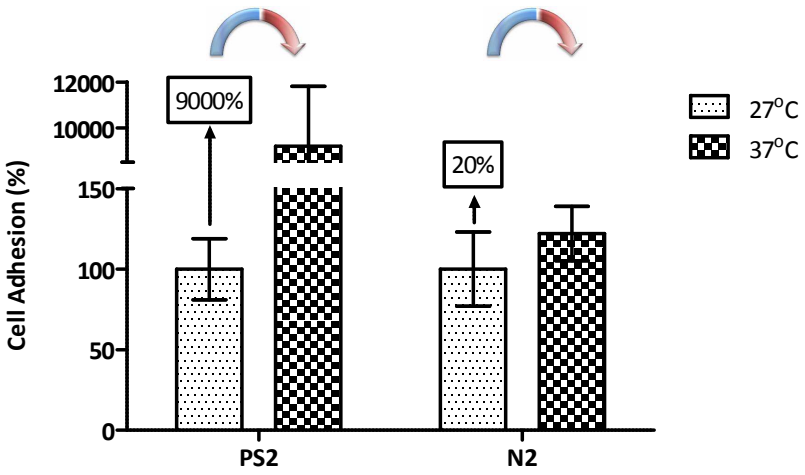

Figure 5.18. Percentage of cell adhesion when the temperature was increased from 27 °C to 37 °C. Tissue cultured polystyrene plates, unmodified (PS2) or modified (N2) with pNIPAAm.

When the temperature was increased from 27 °C to 37 °C different results were presented. In this experiment the samples were first incubated at 27 °C, at this temperature, the cell adhesion was really low because the microorganisms were only metabolically less active and they were growing very slowly. As it was expected, when the temperature was increased, the growth curve for the control (PS2) was exponential (Figure 5.18.). After one incubation hour at

37 ^{o}C, the adhered cells reached a thick biofilm layer that was not observed after incubating cells at 27 ^{o}C. Faced with this result, when the same conditions were applied to the pNIPAAm hydrogel surface, cell adhesion was just increased by 20%. However, cell attachment was greatly reduced in comparison to PS substrates. Such observations may indicate that changes in the structure of the hydrogel can possibly alter proliferation of colonizing microorganisms.

The analyzed films presented different cell adhesion when the temperature was either increased or decreased. The signs of bacterial detachment were visible with naked eye after the phase-transition from 37 ^{o}C to 27 ^{o}C. Top images in Figure 5.19. shows the petri dishes of both films once the second incubation was finished and the samples were washed several times. Bacterial adhesion on the tissue culture plate without modification, left image (a), was higher than on pNIPAAm film. The microorganism created a thick and homogenous layer all over the surface that resembled a biofilm. Different behavior presented by pNIPAAm hydrogel was observed, after the second cultivation, where a significant amount of adhered bacteria started to detach, resulting in a thinner and non-homogeneous biofilm layer.

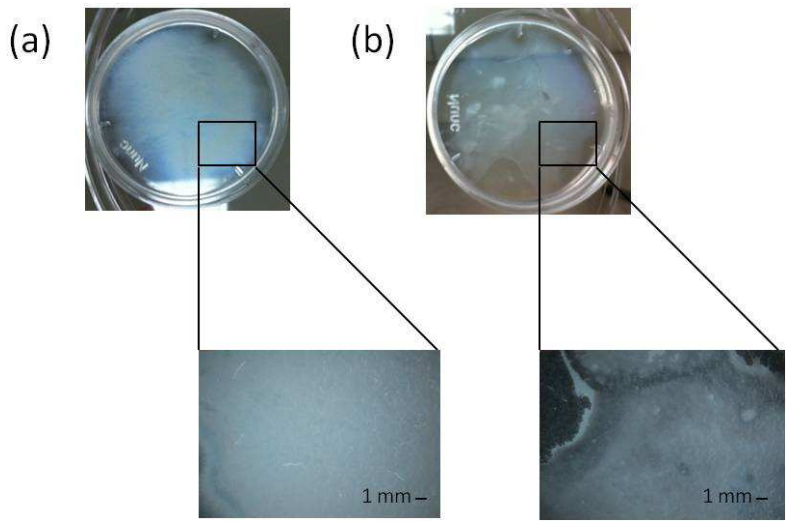

Figure 5.19. Adhered cells on PS (a) and NIPAAm (b).
Cell detachment was observed in NIPAAm hydrogels due to the phase-transition.

5.3.5. Evaluation of the Effect on Bacterial Proliferation of a Drug Released from a Thermo-responsive

As it has been discussed earlier, thermo-responsive hydrogels were originally conceived for the fabrication of smart drug delivery systems. Temperature activates the phase-transition achieving a release system above the LCST. In order to evaluate the potential of thermo-responsive hydrogels as suitable surfaces for embedding antibiotic drugs to control microorganism colonization, pNIPAAm hydrogels were prepared by iCVD, as described in 5.2.1.

In order to increase the anti-biofilm properties of hydrogels deposited by iCVD, a new experiment was designed, where the bacterial resistance of the surfaces was enhance by loading the hydrogel matrix with an antibiotic and taking advantage of the potential controlled release characteristics of this system. Thermo-sensitive hydrogels loaded with hydrophilic drugs are known to release the embedded drug molecules in a sustained way upon heating above the hydrogel LCST.

Tissue culture polystyrene plates, either unmodified or modified with pNIPAAm (PS and NIPAAm samples), were used to embed bacitracin (PS-B and NIPAAm-B). No bacitracin exposed surfaces (PS-O and NIPAAm-O) were used as controls to quantify the effect of the antibiotic. A1 sample (NIPAAm/EGDA - 90/10) was chosen to be deposited on petri dishes due to its sharp phase transition and to correlate the results with experiment 5.2.3. As it has been mentioned, the phase-transition for the A1 hydrogel was around 32 ^{o}C, therefore the incubation temperature was set at 37 ^{o}C to ensure that the hydrogel was in its collapsed state. In addition, earlier experiments revealed that this temperature is optimal for culturing *S. epidermis* (Hola et al. 2006). Briefly, a solution of 1 mM was added to the petri dishes and the samples were cooled to 10 ^{o}C for three hours, and then heated quickly to 37 ^{o}C. After washed the surfaces to

remove the un-loaded drug, bacterial cultures were added and incubated at 37 ^{o}C. At the end of each time-point, bacteria were fully detached from the surfaces by pipetting extensively.

Figure 5.20. shows the amount of bacteria (as colony forming units per milliliter) at 2, 4 and 24 hours for the different surfaces. As it could be observed, in samples without bacitracin (-O), PS-O and NIPAAm-O, bacterial population was dreased in number at 24 hours, when compared to cultures at 4 hours. This phenomenon might be caused by nutritional stress due to starvation of the medium

On the other hand, samples loaded with bacitracin showed a lower bacterial growth rate, indicating that bacitracin was released over the time and was preventing exponential cell growth typically observed for these cultures. PS-B reduced the number of cells, which might caused by the presence of residual bacitracin adhered to the petri dish at the time of bacterial inoculation. No difference between PS-O and PS-B was expected, because no reactions are feasible between PS and bacitracin. It is likely that this behavior is the result of insufficient rinsing after bacitracin loading. The final bacterial concentration for this sample (PS-B, 24h) is in agreement with this idea; bacteria grew up achieving the same value as the PS-O sample.

After 4 hours of incubation a remarkable reduction of the microorganism was observed for NIPAAm-B films, when compared to the other surfaces. These results probably indicate that bacitracin had been released over the course of the experiment and its effect caused the cell death. The increase in bacteria population after the 4th hour probably suggests that all the bacitracin had been delivered or that the amount loaded into the hydrogel was insufficient to kill all the initial bacterial population.

After 24 hours of incubation, the bacteria concentration for NIPAAm hydrogels was up to 70% lower than the population on PS surfaces, even when bacitracin was not present, indicating the high efficacy of this films in antimicrobial applications.

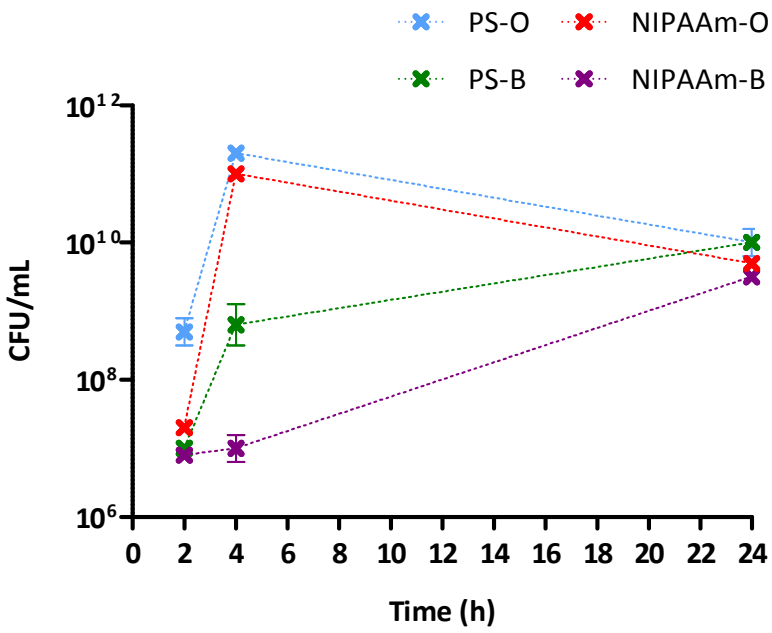

Figure 5.20. Influence of bacitracin on pNIPAAm and PS samples.
Experiments with letter O were the controls and experiments with letter B were the samples that Bacitracin was loaded.

5.4. Discussion

Thermo-responsive hydrogels have been deposited via initiated Chemical Vapor Deposition. Films with a clearly-defined phase-transition were synthesized. The generation of a thermo-sensitive hydrogels library has been developed combining three different components; main acrylamide monomer, different co-monomers and the cross-linker. LCST values of the resulting films can be tunned by combining appropriate ratios of specific monomers

It has been demonstrated that different thermo-responsive hydrogels can be successfully deposited by iCVD. Water Contact Angle analysis confirms wettability changes, when the temperature is increased; surfaces with different hydrophobicity are achieved below and above the LCST. AFM study indicates the roughness of the hydrogels when co-polymers are used during the deposition process. The roughness has been increased adding hydrophilic co-monomers, the hydrophilic nature of these hydrogels generate the appearance of hydrophilic protuberances. This fact has been confirmed with the WCA values.

Phase transition of hydrogels together with their corresponding LCSTs has been determined by Quartz Crystal Microbalance analysis. Previous experiment has been done to correctly determine the phase-transition temperature and to analyze the different factors that has influence on the frequency and the dissipation in QCM-D systems. The effect of the temperature on the experiments has been identified and compensated, and is in good agreement with the results observed in WCA.

QCM-D technique has been also used to determine the behavior of the hydrogels and the influence of the rate of the cross-linker and the nature and the concentration of the co-polymer. The amount of the cross-linker in NIPAAm samples plays an important role in the

phase-transition of the thermo-responsive hydrogels, if the concentration of the cross-linker is higher than 30%, the film is excessively cross-linked to undergo phase-transition. The co-polymerization of NIPAAm with either DMAAm or AAc presents different behavior on the final hydrogel; DMAAm provides a defined transition and causes an increase on the LCST temperature. On the contrary, AAc hydrogel starts the phase transition near low cross-linked NIPAAm (32 ^{o}C) but the process ends around 40 ^{o}C, the use of AAc provides a slow phase-transition, it occurs at a wide range of temperatures.

Finally, to demonstrate the feasibility of these hydrogels as antimicrobial surfaces, proof of concept experiments have been performed with *S. epidermis*. The first experiment was done taking advantage of the capability of these films to change its topography and morphology, when phase-transition is achieved increasing or decreasing the temperature. The results demonstrate high detachment of the microorganism when the temperature was varied from 37 ^{o}C to 27 ^{o}C. Modest increase in bacterial adhesion on NIPAAm film is observed, comparing the results with the control sample, when the temperature was changed from 27 ^{o}C to 37 ^{o}C. The last experiment was done to test the capacity of the films to embed an antibiotic and release it if the temperature increases, that fact will provokes that the hydrogel varied from the swollen to the collapsed state. The experiments reveal a reduction of the 70% in bacteria population when Bacitracin is delivered by NIPAAm films compared to PS surfaces.

Chapter 6.

Conclusions

6.1. Conclusions (English)

It has been demonstrated that piCVD is a gentle method for preparing stable and reversibly swellable hydrogel films with a nanoscale mesh size. The deposition of thin films of pHEMA has been verified by FTIR spectroscopy. The homopolymer deposited in this work enhances the surface resistance to non-specific protein adhesion, as investigated by XPS. An advantage of this process is the ease of forming copolymers, including copolymers of pHEMA, and controlling film composition via the synthetic conditions.

In piCVD, the polymerization occurs primarily on the substrate surface, therefore the cross-link density and subsequently the swelling properties of the film, can be controlled by changing the fractional saturation of the monomer vapor during the deposition. The mesh size of the resulting film is small enough to allow for small analyte molecules to diffuse towards the underlying substrate. This was confirmed by coating a sodium-sensing optode with a thin film of p(HEMA); the optode retained its ability to detect its target analyte. The mild nature of piCVD, which does not require plasma or solvents/which operates without plasma and solvents, makes it ideal for coating the surfaces of delicate medical devices, such as optodes and other sensors designed for implantation.

It has been demonstrated that both homogeneous and graded copolymers can be successfully deposited by piCVD. FTIR and ToF-SIMS analyses confirm that the reactive pentafluorphenyl ester group (PFM) is conserved during the photopolymerization, allowing for the formation of thin films capable of post-functionalization with primary amines. The controlled distribution of PFM within the film matrix has also been confirmed. In the graded co-polymer films, the PFM

signals in both XPS and ToF-SIMS decrease from a maximum at the top surface, confirming the nano-confinement of the reactive moiety at the near-surface region.

There are two key benefits derived from the material properties when targeting near-surface confinement. First, the hydrogel properties of the bulk region of graded copolymers are largely maintained. This is especially important when compared to the homogeneous copolymers, which exhibit markedly reduced swelling properties. For the graded films, the underlying properties of the homopolymer can be chosen independently from the properties of the surface activity. Second, nearly all the PFM moieties in the graded copolymer are available for reaction. In the homogeneous copolymer, much of the PFM remains buried within the polymer matrix. It should be noted that any vinyl comonomer capable of being introduced into the reactor as a vapor can be used to form the graded functional film.

The here presented micro-patterning technique presented not only allows the fabrication of topographic reliefs in a fast and efficient way, but it also enables the design of 3D features having defined spatial chemical patterns. Careful choice of suitable monomers should allow the design of surfaces having special features, such as wetting behavior, anti-biofouling activity or cell attachment, among others.

A new method to increase the mechanical stability of electrodeposited black platinum on biosensors has been presented. The thin hydrogel layer of deposited pHEMA does not interfere with the passage of the analytes and is conformal to the black platinum coating. Moreover, the deposited film slightly decreases the impedance module of the sensor, resulting in improvement of the sensor performance. The deposited hydrogel is chemically inert and protects the black platinum layer against mechanical damage, allowing a continuous use of the

biosensor in contact with living tissues. This results in a better sensor performance as shown *in vivo* experiments.

It has been demonstrated that iCVD is a feasible method for preparing stable and thermo-sensible thin hydrogel films. A library of thermo-sensitive films has been developed by combining three different components; main acrylamide monomer, different co-monomers and the cross-linker. The study of the hydrogels properties, depending on their composition, has been monitored by QCM-D analysis to determine the LCST temperature.

The use of cross-linked NIPAAm film enhances the surface resistance against bacterial adhesion. The capability of the hydrogels to change the topography and the morphology during the phase transition detaches bacteria from the surfaces. Another study has revealed the possibility to embed an antibiotic and release it, when the temperature increases; the combination of the thermo-responsive film properties opens the possibility to design tunable and reversible coatings to manage biofilm formation.

6.2. Conclusions (Català)

S'ha demostrat que el piCVD és un bon mètode per preparar pel·lícules d'hidrogel que siguin estables, amb una capacitat controlada d'incorporar aigua de forma reversible i amb un mida de malla nanomètrica de malla. La deposició del films de pHEMA s'ha verificat mitjançat espectrometria FTIR. L'homopolímer dipositat en aquest treball millora la resistència a l'adhesió no específica de proteïnes mitjançant anàlisi d'XPS. Una avantatge d'aquest procés és la facilitat de formar co-polímers, inclosos els copolímers de HEMA, i controlar la composició del film mitjançant les condicions experimentals.

La polimerització amb piCVD succeeix en primer lloc a la superfície del substrat, i la densitat de reticulació, i per tant la capacitat d'absorbir aigua del film, pot ser controlada tot canviant la pressió de saturació pròpia del monòmer durant la deposició. La pel·lícula té un grau de reticulació prou petit com per permetre la difusió de petites molècules a través del film. Aquest fenomen s'ha confirmat recobrint un sensor òptic de sodi amb un film de pHEMA. Després del recobriment, el sensor reté la seva capacitat de detectar l'analit d'estudi. La naturalesa no agressiva, al no utilitzar ni plasma ni dissolvent, del piCVD el fa ideal per recobrir les superfícies dels sensors òptics i altres sensors dissenyats per a ser implantats.

S'ha demostrat que es poden dipositar per piCVD co-polímers homogenis i de concentració gradual de forma satisfactòria. Anàlisis de FTIR i ToF-SIMS confirmen que el grup éster reactiu del PFM es manté intacte després de la deposició via piCVD, permetent la formació de pel·lícules capaces de ser post-funcionalitzades amb amines primàries. La distribució de PFM en el gruix del film també s'ha confirmat. En el copolímer de concentració gradual, les senyals de PFM tant de l'XPS com del ToF-SIMS disminueixen al allunyar-se de la superficie, trobant-se

el màxim a la superfície de la pel·lícula. D'aquesta manera es confirma que la zona reactiva es troba a la part més superficial del film.

Existeixen dos beneficis principals d'aquesta nano-estructuració polimèrica. El primer és que les propietats de l'hidrogel es mantenen en el cas del co-polímer de concentració gradual. Aquest fet és especialment important quan es compara amb els co-polímers homogenis, els quals exhibeixen una menor capacitat d'absorbir aigua, perdent d'aquesta manera el seu caràcter d'hidrogel.

Per les pel·lícules no homogènies, les propietats de les capes més internes de l'homopolímer es poden escollir independentment de l'activitat superficial. El segon avantatge és que gairebé totes les parts reactives del PFM en el copolímer de concentració gradual són accessibles per reaccionar. En canvi, en el copolímer homogeni, la majoria d'aquests punts reactius estan atrapades a l'interior de la matriu polimèrica. Val a dir que qualsevol co-monòmer vinílic capaç de ser introduït en un reactor en estat vapor pot ser utilitzat per formar un co-polímer de concentració gradual.

La tècnica de micro-estructuració presentada no només permet la fabricació de superfícies amb relleu de manera ràpida i fàcil, sinó que també permet fer un disseny 3D per poder tenir estructures químiques definides. Tenint especial cura amb la elecció dels monòmers utilitzats, es poden dissenyar superfícies amb característiques determinades, comportaments humectants, activitats anti-fouling o adherència de cèl·lules, entre d'altres.

S'ha estudiat un nou mètode per incrementar la estabilitat del platí negre dipositat electroquímicament sobre biosensors. La deposició de pel·lícules de pHEMA permet que l'analit travessi el film i s'ajusta a la topografia del platí negre. A més a més, s'ha vist com la

deposició del film disminueix la mesura d'impedància, millorant d'aquesta manera el comportament del sensor. La capa d'hidrogel és totalment inert i protegeix la pel·lícula de platí negre de les agressions mecàniques, permetent fer un ús continuat dels biosensors sobre organismes vius.

S'ha comprovat que l'iCVD es un bon mètode per preparar pel·lícules d'hidrogel que siguin estables i termo-sensibles. S'ha desenvolupat una llibreria de films termo-sensibles combinant tres components: una acrilamida com a monòmer principal, diferents copolímers i un agent reticulant. L'estudi de les propietats dels hidrogels i la influencia de la seva composició s'ha estudiat amb una microbalança QCM-D per determinar la temperatura LCST.

L'ús d'un film de pNIPAAm millora la resistència de les superfícies contra l'adhesió bacteriana. La capacitat dels hidrogels per modificar la seva topografia i morfologia durant la fase de transició, permet desadherir les bactèries de la superfície. Un altre estudi va revelar la possibilitat de emmagatzemar un antibiòtic dins la matriu de l'hidrogel i expulsar-lo quan al augmentar la temperatura. La combinació de les propietats que ofereixen els hidrogels termo-sensibles obre la porta per dissenyar recobriments ajustables i reversibles per controlar la formació de biofilms.

Chapter 7.

References

Abraham, S. et al., 2005. Molecularly engineered p(HEMA)-based hydrogels for implant biochip biocompatibility. *Biomaterials*, 26(23), pp.4767-78.

Abrahams, E.W., Littler, J.G. & Vo, P., 1966. Spectroscopic Basis of Carbonyl Photochemistry. I. The Role of Excited-State Geometry in the Photodecomposition of Formaldehyde. *Journal of Chemical Physics*, 44(11), pp.4082-4086.

Abulateefeh, S.R. et al., 2011. Thermoresponsive Polymer Colloids for Drug Delivery and Cancer Therapy. *Macromolecular Bioscience*, 11(12), pp.1722-1734.

Adamson, A.W. & Gast, A.P., 1997. *Physical Chemistry of Surfaces*, NY: John Wiley & Sons, Inc.

Adden, N. et al., 2006. Synthesis and Characterization of Biocompatible Polymer Interlayers on Titanium Implant Materials. *Biomacromolecules*, 7(9), pp.2552-2559.

Adiga, S.P. et al., 2008. Nanoporous Materials for Biomedical Devices. , (March).

Adiga, S.P. & Brenner, D.W., 2012. Stimuli-Responsive Polymer Brushes for Flow Control through Nanopores. *Journal of Functional Biomaterials*, 3(2), pp.239-256.

Aguilar, M.R. et al., 2007. Smart Polymers and Their Applications as Biomaterials. *Topics in Tissue Engineering*, 3, pp.1-27.

Akovali, G. et al., 1998. Mechanical properties and surface energies of low density polyethylene-poly(vinyl chloride) blends. *Polymer*, 39(6–7), pp.1363-1368.

Alam, M., Miah, M. & Ahmad, H., 2007. Composite polymer particles with stimuli-responsive surface properties and specific activity of adsorbed/released trypsin. *Colloid & Polymer Science*, 285(6), pp.715-720.

Alf, M.E., Hatton, T.A. & Gleason, K.K., 2011. Novel N-isopropylacrylamide based polymer architecture for faster LCST transition kinetics. *Polymer*, 52(20), pp.4429-4434.

Bajpai, A. & Kankane, S., 2008. Evaluation of water sorption property and in vitro blood compatibility of poly(2-hydroxyethyl methacrylate) (PHEMA) based semi interpenetrating polymer networks (IPNs). *Journal of Materials Science: Materials in Medicine*, 19(5), pp.1921-1933.

Bard, A.J. & Faulkner, L.R., 2001. *Electrochemical methods: fundamentals and applications*, New York: Wiley.

Baxamusa, S.H. et al., 2008. Protection of sensors for biological applications by photoinitiated chemical vapor deposition of hydrogel thin films. *Biomacromolecules*, 9(10), pp.2857-62.

Baxamusa, S.H. & Gleason, K.K., 2008a. Thin Polymer Films with High Step Coverage in Microtrenches by Initiated CVD. *Chemical Vapor Deposition*, 14(9-10), pp.313-318.

Baxamusa, S.H. & Gleason, K.K., 2008b. chemical vapor deposition. *Chemical Vapor Deposition*, p.in press.

Baxamusa, S.H., Im, S.G. & Gleason, K.K., 2009. Initiated and oxidative chemical vapor deposition: a scalable method for conformal and functional polymer films on real substrates. *Physical chemistry chemical physics : PCCP*, 11(26), pp.5227-40.

Bayramoglu, G. & Arica, M.Y., 2005. Surface energy components of a dye-ligand immobilized pHEMA membranes: Effects of their molecular attracting forces for non-covalent interactions with IgG and HSA in aqueous media. *International Journal of Biological Macromolecules*, 37(5), pp.249-256.

Beh, W.S. et al., 1999. Formation of Patterned Microstructures of Conducting Polymers by Soft Lithography, and Applications in Microelectronic Device Fabrication. *Advanced Materials*, 11(12), pp.1038-1041.

Bures, P. et al., 2001. Surface modifications and molecular imprinting of polymers in medical and pharmaceutical applications. *Journal of controlled release : official journal of the Controlled Release Society*, 72(1-3), pp.25-33.

Byfield, M.P. & Abuknesha, R.A., 1994. biochemical aspects of biosensors. *Biosensors & bioelectronics*, 9, pp.373-400.

Böker, A. et al., 2003. Electric Field Induced Alignment of Concentrated Block Copolymer Solutions. *Macromolecules*, 36(21), pp.8078-8087.

Canal, T. & Peppas, N.A., 1989. Correlation between mesh size and equilibrium degree of swelling of polymeric networks. *Journal of Biomedical Materials Research*, 23(10), pp.1183-1193.

Chan, K. & Gleason, K.K., 2005a. Initiated CVD of Poly(methyl methacrylate) Thin Films. *Chemical Vapor Deposition*, 11(10), pp.437-443.

Chan, K. & Gleason, K.K., 2005b. Initiated Chemical Vapor Deposition of Linear and Cross-linked Poly(2-hydroxyethyl methacrylate) for Use as Thin-Film Hydrogels. *Langmuir*, 21(19), pp.8930-8939. Available at: http://www.ncbi.nlm.nih.gov/pubmed/16142981.

Chen, W. & Mccarthy, T.J., 1997. Layer-by-Layer Deposition : A Tool for Polymer Surface Modification. *Macromolecular Symposia*, 30(1), pp.78-86.

Chilkoti, A. et al., 1993. Analysis of polymer surfaces by SIMS. 16. Investigation of surface crosslinking in polymer gels of 2-hydroxyethyl methacrylate. *Macromolecules*, 26(18), pp.4825-4832.

Chirila, T.V. et al., 1993. Poly(2-hydroxyethyl methacrylate) sponges as implant materials: in vivo and in vitro evaluation of cellular invasion. *Biomaterials*, 14(1), pp.26-38.

Cho, S.B. & Thielecke, H., 2005. Design of electrode array for impedance measurement of lesions in arteries. *Physiological Measurement*, 26(2, SI), p.S19-S26.

Chu, L., XIE, R. & JU, X., 2011. Stimuli-responsive Membranes: Smart Tools for Controllable Mass-transfer and Separation Processes. *Chinese Journal of Chemical Engineering*, 19(6), pp.891-903.

Clark, H.A. et al., 1999. Optical Nanosensors for Chemical Analysis inside Single Living Cells. 1. Fabrication, Characterization, and Methods for Intracellular Delivery of PEBBLE Sensors. *Analytical Chemistry*, 71(21), pp.4831-4836.

Cogan, S.F., 2008. Neural stimulation and recording electrodes. *Annual review of biomedical engineering*, 10, pp.275-309.

Cole, M.A. et al., 2009. Stimuli-responsive interfaces and systems for the control of protein–surface and cell–surface interactions. *Biomaterials*, 30(9), pp.1827-1850.

Corkhill, P.H., Hamilton, C.J. & Tighe, B.J., 1989. Synthetic hydrogels VI. Hydrogel composites as wound dressings and implant materials. *Biomaterials*, 10(1), pp.3-10.

Cunliffe, D. et al., 2003. Thermoresponsive Surface-Grafted Poly(N−isopropylacrylamide) Copolymers: Effect of Phase Transitions on Protein and Bacterial Attachment. *Langmuir*, 19(7), pp.2888-2899.

Davidson, J.L., 2004. *Microfabricated Systems and MEMS VII: Proceedings of the International Symposium*, The Electrochemical Society.

Deshmukh, S. et al., 2009. Photoresponsive Behavior of Amphiphilic Copolymers of Azobenzene and N,N-Dimethylacrylamide in Aqueous Solutions. *Langmuir*, 25(6), pp.3459-3466.

Discher, D.E., Janmey, P. & Wang, Y.L., 2005. Tissue Cells Feel and Respond to the Stiffness of Their Substrate. *Science*, 310(5751), pp.1139-1143.

Dubach, J.M., Harjes, D.I. & Clark, H.A., 2007a. Fluorescent Ion-Selective Nanosensors for Intracellular Analysis with Improved Lifetime and Size. *Nano Letters*, 7(6), pp.1827-1831.

Dubach, J.M., Harjes, D.I. & Clark, H.A., 2007b. Ion-Selective Nano-optodes Incorporating Quantum Dots. *Journal of the American Chemical Society*, 129(27), pp.8418-8419.

von Eiff, C. et al., 2005. Infections associated with medical devices: pathogenesis, management and prophylaxis. *Drugs*, 65(2), pp.179-214.

Elbert, D.L. & Hubbell, J.A., 1996. SURFACE TREATMENTS OF POLYMERS FOR B IOCOMPATIBILITY. *Annual review Material Science*, 26, pp.294-365.

Elman, N.M. et al., 2009. The Next Generation of Drug-Delivery Microdevices. *Clin Pharmacol Ther*, 85(5), pp.544-547.

Emr, S.A. & Yacynych, A.M., 1995. Use of polymer films in amperometric biosensors. *Electroanalysis*, 7(10), pp.913-923.

Favia, P. et al., 2003. Novel plasma processes for biomaterials: micro-scale patterning of biomedical polymers. *Surface and Coatings Technology*, 169–170(0), pp.707-711.

Feng, C.L. et al., 2005. Reactive Thin Polymer Films as Platforms for the Immobilization of Biomolecules. *Biomacromolecules*, 6(6), pp.3243-3251.

Feng, M., 1996. Adsorption of High Density Lipoproteins (HDL) on Solid Surfaces. *Journal of Colloid and Interface Science*, 177(2), pp.364-371.

Ferguson, J.E., Boldt, C. & Redish, D., 2009. Creating low-impedance tetrodes by electroplating with additives. *Sensors and actuators. A, Physical*, 156(2), pp.388-393.

Folkman, J. & Moscona, A., 1978. Role of cell shape in growth control. *Nature*, 273(5661), pp.345-349.

Francesch, L. et al., 2005. Fabrication of Bioactive Surfaces by Plasma Polymerization Techniques Using a Novel Acrylate-Derived Monomer. *Plasma Processes and Polymers*, 2(8), pp.605-611.

Francesch, L., 2008. *Surface modification of polymers by plasma polymerization techniques for tissue engineering*. Universitat Ramon Llull.

Francesch, L. et al., 2007. Surface reactivity of pulsed-plasma polymerized pentafluorophenyl methacrylate (PFM) toward amines and proteins in solution. *Langmuir the ACS journal of surfaces and colloids*, 23(7), pp.3927-31.

Gabriel, G. et al., 2009. Easily made single-walled carbon nanotube surface microelectrodes for neuronal applications. *Biosensors & bioelectronics*, 24(7), pp.1942-8.

Gabriel, G. et al., 2007. Manufacturing and full characterization of silicon carbide-based multi-sensor micro-probes for biomedical applications. *Microelectronics Journal*, 38(3), pp.406-415.

Gabriel, G. et al., 2008. Single-walled carbon nanotubes deposited on surface electrodes to improve interface impedance. *Physiological measurement*, 29(6), pp.S203-12.

Gamry Instruments, 2012. Basics of a Quartz Crystal Microbalance. , p.5.

Garreta, E., 2005. *Development of Biomaterials fo bone tissue engineering*. Universitat Ramon Llull.

Garrod, R.P. et al., 2006. Mimicking a Stenocara Beetle's Back for Microcondensation Using Plasmachemical Patterned Superhydrophobic−Superhydrophilic Surfaces. *Langmuir*, 23(2), pp.689-693.

Gates, B.D. et al., 2005. New Approaches to Nanofabrication: Molding, Printing, and Other Techniques. *Chemical Reviews*, 105(4), pp.1171-1196.

Gavalas, V., Berrocal, M. & Bachas, L., 2006. Enhancing the blood compatibility of ion-selective electrodes. *Analytical and Bioanalytical Chemistry*, 384(1), pp.65-72.

Geismann, C. & Ulbricht, M., 2005. Photoreactive Functionalization of Poly(ethylene terephthalate) Track-Etched Pore Surfaces with "Smart" Polymer Systems. *Macromolecular Chemistry and Physics*, 206(2), pp.268-281.

Giacomelli, F.C. et al., 2010. Cubic to Hexagonal Phase Transition Induced by Electric Field. *Macromolecules*, 43(9), pp.4261-4267.

Goessl, A. et al., 2001. Plasma lithography — thin-film patterning of polymeric biomaterials by RF plasma polymerization I: Surface preparation and analysis. *Journal of biomaterials Science, Polymer edition*, 12(7), pp.721-738.

Gooding, J.J., 2005. Nanostructuring electrodes with carbon nanotubes: A review on electrochemistry and applications for sensing. *Electrochimica Acta*, 50(15, SI), pp.3049-3060.

Gorbet, M.B. & Sefton, M.V., 2004. Biomaterial-associated thrombosis: roles of coagulation factors, complement, platelets and leukocytes. *Biomaterials*, 25(26), pp.5681-5703.

Grimnes, S. & Grottem, O., 2008. *Bioimpedance and Bioelectricity Basics*, Academic Press.

Grimnes, S. & Martinsen, O.G., 2007. Sources of error in tetrapolar impedance measurements on biomaterials and other ionic conductors. *Journal of Physics D-Applied Physics*, 40(1), pp.9-14.

Gründler, P., 2007. *Chemical Sensors* Springer, ed.,

Guimera, A. et al., 2008. Method and device for bio-impedance measurement with hard-tissue applications. *Physiological Measurement*, 29(6, SI), p.S279-S290.

Gupta, M. & Gleason, K.K., 2006. Initiated Chemical Vapor Deposition of Poly(1H,1H,2H,2H-perfluorodecyl Acrylate) Thin Films. *Langmuir*, 22(24), pp.10047-10052.

Harant, A.W. et al., 2005. Micropatterning organosilane serlf-assembled monolayers with plasma etching and backfilling techniques. *Journal of Vacuum Science & Technology B*, 23(2), p.354.

Heer, F. et al., 2004. CMOS microelectrode array for the monitoring of electrogenic cells. *Biosensors & bioelectronics*, 20(2), pp.358-366.

Heim, M., Yvert, B. & Kuhn, A., 2011. Nanostructuration strategies to enhance microelectrode array (MEA) performance for neuronal recording and stimulation. *Journal of physiology, Paris*, pp.1-9.

Hirano, Y. & Mooney, D.J., 2004. Peptide and Protein Presenting Materials for Tissue Engineering. *Advanced Materials*, 16(1), pp.17-25.

Hola, V., Rucicka, F. & Votava, M., 2006. The dynamics of staphylococcus epidermis biofilm formaTion in relaTion To nuTriTion , TemperaTure , and Time. *Scripta medica (BRNO)*, 79(3), pp.169-174.

Huang, X.J., O'Mahony, A.M. & Compton, R.G., 2009. Microelectrode Arrays for Electrochemistry: Approaches to Fabrication. *Small*, 5(7), pp.776-788.

Hubbell, J. a, 1999. Bioactive biomaterials. *Current opinion in biotechnology*, 10(2), pp.123-9.

Hubbell, J.A., 1995. Biomaterials in Tissue Engineering. *Nature biotechnology*, 13, pp.565-576.

Humblot, V. et al., 2009. The antibacterial activity of Magainin I immobilized onto mixed thiols Self-Assembled Monolayers. *Biomaterials*, 30(21), pp.3503-12.

Hussain, A.A. et al., 2008. Prediction of physical properties of nanofiltration membranes using experiment and theoretical models. *Journal of Membrane Science*, 310(1–2), pp.321-336.

Ikada, Y., 1994. Surface modification of polymers for medical applications. *Biomaterials*, 15(10), pp.725-36.

Im, S.G. et al., 2008. Patterning Nanodomains with Orthogonal Functionalities: Solventless Synthesis of Self-Sorting Surfaces. *Journal of the American Chemical Society*, 130(44), pp.14424-14425.

Ishida, N. & Biggs, S., 2007. Direct Observation of the Phase Transition for a Poly(N-isopropylacryamide) Layer Grafted onto a Solid Surface by AFM and QCM-D. *Langmuir*, 23(22), pp.11083-11088.

Ista, L., Mendez, S. & Lopez, G., 2010. Attachment and detachment of bacteria on surfaces with tunable and swithable wettability. *Biofouling*, 26(1), pp.111-118.

Ivorra, A. et al., 2003. Minimally invasive silicon probe for electrical impedance measurements in small animals. *Biosensors & bioelectronics*, 19(4), pp.391-399.

Iwata, H., Hirata, I. & Ikada, Y., 1998. Atomic Force Microscopic Analysis of a Porous Membrane with pH-Sensitive Molecular Valves. *Macromolecules*, 31(11), pp.3671-3678.

James M, A., 1993. Chapter 4 Mechanisms of inflammation and infection with implanted devices. *Cardiovascular Pathology*, 2(3, Supplement), pp.33-41.

Janacek, J. & Hassa, J., 1966. No Title. *journal collection of czechoslovak chemical communications*, 31, pp.2186-2200.

Janders, M., Egert, U. & Stelze, M., 1996. Novel thin film titanium nitride micro-electrodes with excellent charge transfer capability for cell stimulation and sensing applications. *18th Annual International Conference of the IEEE Engineering in Medicine and Biology Society*.

Jhon, Y.K. et al., 2006. Salt-Induced Depression of Lower Critical Solution Temperature in a Surface-Grafted Neutral Thermoresponsive Polymer. *Macromolecular Rapid*

Communications, 27(9), pp.697-701. Available at: http://doi.wiley.com/10.1002/marc.200600031 [Accessed April 18, 2012].

Johnson, A.M. et al., 2005. Design and Testing of an Impedance-Based Sensor for Monitoring Drug Delivery. *Journal of The Electrochemical Society*, 152(1), p.H6.

Jones, D.S., Djokic, J. & Gorman, S.P., 2005. The resistance of polyvinylpyrrolidone–Iodine–poly(ε-caprolactone) blends to adherence of Escherichia coli. *Biomaterials*, 26(14), pp.2013-2020.

Keefer, E.W. et al., 2008. Carbon nanotube coating improves neuronal recordings. *Nature Nanotechnology*, 3(7), pp.434-439.

Krüss, http://www.kruss.de/en/products/contact-angle/dsa100.html. 20/03/2012.

Laloyaux, X. et al., 2010. Surface and bulk collapse transitions of thermoresponsive polymer brushes. *Langmuir : the ACS journal of surfaces and colloids*, 26(2), pp.838-47.

Lau, K.K.S. et al., 2003. Fluorocarbon dielectrics via hot filament chemical vapor deposition. *Journal of Fluorine Chemistry*, 122(1), pp.93-96.

Lau, K.K.S. & Gleason, K.K., 2006. Initiated Chemical Vapor Deposition (iCVD) of Poly (alkyl acrylates): A Kinetic Model. *Macromolecules*, 39(10), pp.3695-3703.

Lau, K.K.S. & Gleason, K.K., 2008. Initiated chemical vapor deposition (iCVD) of copolymer thin films. *Thin Solid Films*, 516(5), pp.678-680.

Lee, J. et al., 2002. Negative-working photoresist of methacrylate polymers based on the transesterification of the 2-hydroxyethyl group in the presence of an acid. *Journal of Polymer Science Part A: Polymer Chemistry*, 40(11), pp.1858-1867.

Lee, K.Y., Bouhadir, K.H. & Mooney, D.J., 2004. Controlled degradation of hydrogels using multi-functional cross-linking molecules. *Biomaterials*, 25(13), pp.2461-2466.

Leobandung, W. et al., 2002. Preparation of stable insulin-loaded nanospheres of poly(ethylene glycol) macromers and N-isopropyl acrylamide. *Journal of controlled release : official journal of the Controlled Release Society*, 80(1-3), pp.357-63. Available at: http://www.ncbi.nlm.nih.gov/pubmed/11943411.

Lewis, H.G.P., Caulfield, J.A. & Gleason, K.K., 2001. Perfluorooctane Sulfonyl Fluoride as an Initiator in Hot-Filament Chemical Vapor Deposition of Fluorocarbon Thin Films. *Langmuir*, 17(24), pp.7652-7655.

Li, Y.Y. et al., 2003. Polymer Replicas of Photonic Porous Silicon for Sensing and Drug Delivery Applications. *Science*, 299(5615), pp.2045-2047.

Lin-Vien, D., Fately, N.C.W. & Grasselli, J., 1991. *The Handbook of Infrared and Raman Characteristic Frequencies of Organic Molecules*, San Diego, CA: Academic Press.

Lloyd, A.W., Faragher, R.G.A. & Denyer, S.P., 2001. Ocular biomaterials and implants. *Biomaterials*, 22(8), pp.769-785.

Loeb, G.E., Peck, R.A. & Martyniuk, J., 1995. Toward the ultimate metal microelectrode. *Journal of neural engineering*, 63(1-2), pp.175-183.

Lokuge, I., Wang, X. & Bohn, P.W., 2006. Temperature-Controlled Flow Switching in Nanocapillary Array Membranes Mediated by Poly(N-isopropylacrylamide) Polymer Brushes Grafted by Atom Transfer Radical Polymerization†. *Langmuir*, 23(1), pp.305-311.

Lopez, G.P. et al., 1993. Plasma deposition of ultrathin films of poly(2-hydroxyethyl methacrylate): surface analysis and protein adsorption measurements. *Macromolecules*, 26(13), pp.3247-3253.

Lou, X. et al., 2006. Radical polymerization in biosensing. *Analytical and Bioanalytical Chemistry*, 386(3), pp.525-531.

Lucht, L.M. & Peppas, N.A., 1981. *Crosslinked macromolecular structures in bituminous coals: Theoretical and eperimental considerations. In Chemistry and Physics of Coal Utilization* B. S. Cooper & L. Petrakis, eds., New York, NY: American Institute of Physics.

Ludwig, K.A. et al., 2006. Chronic neural recordings using silicon microelectrode arrays electrochemically deposited with a poly(3,4-ethylenedioxythiophene) (PEDOT) film. *Journal of neural engineering*, 3(1), pp.59-70.

Ma, H. et al., 2009. Real-time measurement of the mass of water expelled by poly(N-isopropylacrylamide) brushes upon thermo-induced collapse. *Chemical Communications*, (23), pp.3428-3430.

Maki K, H., 2007. Controlled biological and biomimetic systems for landmine detection. *Biosensors and Bioelectronics*, 23(1), pp.1-18.

Malkov, G.S. et al., 2008. Pulsed-Plasma-Induced Micropatterning with Alternating Hydrophilic and Hydrophobic Surface Chemistries. *Plasma Processes and Polymers*, 5(2), pp.129-145.

Mao, Y. & Gleason, K.K., 2004. Hot filament chemical vapor deposition of poly(glycidyl methacrylate) thin films using tert-butyl peroxide as an initiator. *Langmuir the ACS journal of surfaces and colloids*, 20(6), pp.2484-8.

Marrese, C.A., 1987. PREPARATION OF STRONGLY ADHERENT PLATINUM BLACK COATINGS. *Analytical Chemistry*, 59(1), pp.217-218.

Martin, T.P., Chan, K. & Gleason, K.K., 2008. Combinatorial initiated chemical vapor deposition (iCVD) for polymer thin film discovery. *Thin Solid Films*, 516(5), pp.681-683.

Martin-Fernandez, I. et al., 2009. Vertically aligned multi-walled carbon nanotube growth on platinum electrodes for bio-impedance applications. *Microelectronic Engineering*, 86(4-6), pp.806-808.

Martins, M.C.L. et al., 2003. Albumin and fibrinogen adsorption on PU-PHEMA surfaces. *Biomaterials*, 24(12), pp.2067-2076.

Miller et al., 2002. Direct printing of polymer microstructures on flat and spherical surfaces using letterpress technique. , 20(6), p.2320.

Montero, L. et al., 2009. Thin Hydrogel Films With Nanoconfined Surface Reactivity by Photoinitiated Chemical Vapor Deposition. *Chemistry of Materials*, 21(2), pp.399-403.

Morra, M. & Cassinelli, C., 1995. Surface field of forces and protein adsorption behavior of poly(hydroxyethylmethacrylate) films deposited from plasma. *Journal of Biomedical Materials Research*, 29(1), pp.39-45.

Muguruma, H., 2007. Plasma-polymerized films for biosensors II. *TrAC Trends in Analytical Chemistry*, 26(5), pp.433-443.

Murthy, R. et al., 2007. Protein-Resistant Silicones: Incorporation of Poly(ethylene oxide) via Siloxane Tethers. *Biomacromolecules*, 8(10), pp.3244-3252.

Murthy, S.K., Olsen, B.D. & Gleason, K.K., 2002. Initiation of Cyclic Vinylmethylsiloxane Polymerization in a Hot-Filament Chemical Vapor Deposition Process. *Langmuir*, 18(16), pp.6424-6428.

Negi, S. et al., 2010. In vitro comparison of sputtered iridium oxide and platinum-coated neural implantable microelectrode arrays. *Biomedical Materials*, 5(1).

Ng, C.O. & Tighe, B.J., 1976. Polymers in contact lens applications VI. The "dissolved" oxygen permeability of hydrogels and the design of materials for use in continuous-wear lenses. *British Polymer Journal*, 8(4), pp.118-123.

Nichols, R.L. & Raad, I.I., 1999. Management of bacterial complications in critically ill patients: surgical wound and catheter-related infections. *Diagnostic Microbiology and Infectious Disease*, 33(2), pp.121-130.

Nie, Z. & Kumacheva, E., 2008. Patterning surfaces with functional polymers. *Nat Mater*, 7(4), pp.277-290.

Olsson, A.L.J. et al., 2009. Influence of cell surface appendages on the bacterium-substratum interface measured real-time using QCM-D. *Langmuir the ACS journal of surfaces and colloids*, 25(3), pp.1627-32.

Ozaydin Ince, G. & Gleason, K.K., 2010. Tunable Conformality of Polymer Coatings on High Aspect Ratio Features. *Chemical Vapor Deposition*, 16(1-3), pp.100-105.

Ozaydin Ince, G., Gleason, K.K. & Demirel, M.C., 2011. A stimuli-responsive coaxial nanofilm for burst release. *Soft Matter*, 7(2), p.638.

O'Shaughnessy, W.S. et al., 2007. Initiated Chemical Vapor Deposition of a Surface-Modifiable Copolymer for Covalent Attachment and Patterning of Nucleophilic Ligands. *Macromolecular Rapid Communications*, 28(18-19), pp.1877-1882.

Paik, S.J., Park, Y. & Cho, D.I., 2003. Roughened polysilicon for low impedance microelectrodes in neural probes. *Journal of Micromechanics and microengineering*, 13(3), pp.373-379.

Pan, K. et al., 2010. Double stimuli-responsive membranes grafted with block copolymer by ATRP method. *Journal of Membrane Science*, 356(1–2), pp.133-137.

Pappenheimer, J.R., Renkin, E.M. & Borrero, M.L., 1951. Filtration, Diffusion and Molecular Sieving Through Peripheral Capillary Membranes: A Contribution to the Pore Theory of Capillary Permeability. *American journal phyisiology*, 167(1), pp.13-46.

Park, E.J., Draper, D.D. & Flynn, N.T., 2007. Adsorption and thermoresponsive behavior of poly(N-isopropylacrylamide-co-N,N'-cystaminebisacrylamide) thin films on gold. *Langmuir the ACS journal of surfaces and colloids*, 23(13), pp.7083-9.

Park, Y.S., Ito, Y. & Imanishi, Y., 1998. Photocontrolled Gating by Polymer Brushes Grafted on Porous Glass Filter. *Macromolecules*, 31(8), pp.2606-2610.

Parker, A.R. & Lawrence, C.R., 2001. Water capture by a desert beetle. *Nature*, 414(6859), pp.33-34.

Peppas, N.A. et al., 2000. Physicochemical foundations and structural design of hydrogels in medicine and biology. *Annual review of biomedical engineering*, 2, pp.9-29.

Peppas, N.A. & Brannon-Peppas, L., 1990. Hydrogels at critical conditions. Part 1. Thermodynamics and swelling behavior. *Journal of Membrane Science*, 48(2-3), pp.281-290.

Peppas, N.A., Moynihan, H.J. & Lucht, L.M., 1985. The structure of highly crosslinked poly(2-hydroxyethyl methacrylate) hydrogels. *Journal of Biomedical Materials Research*, 19(4), pp.397-411.

Peppas, N.A. & Yang, W.H.M., 1981. Properties Based Optimization of the Structure of Polymers for Contact Lens Applications. *Contact & Intraocular Lens Medical Journal*, 7(4), pp.300-314.

Pierson, H.O., 1999. *Handbook of chemical vapor depostion: principles, technology, and applications*, NY: Elsevier.

Priano, G. et al., 2008. Disposable gold electrode array for simultaueous electrochemical studies. *Electroanalysis*, 20(1), pp.91-97.

QSense, www.q-sense.com. 15/03/2012.

Quinn, C.A.P., Connor, R.E. & Heller, A., 1997. Biocompatible, glucose-permeable hydrogel for in situ coating of implantable biosensors. *Biomaterials*, 18(24), pp.1665-1670.

Rajinder S, S., 1994. Transducer aspects of biosensors. *Biosensors and Bioelectronics*, 9(3), pp.243-264.

Von Recum, A. & Jacobi, J.E., 1999. *Handbook of biomaterials evaluation* Andreas Von Recum, ed., Taylor & Francis.

Robinson, D.A., 1968. OCULOMOTOR CONTROL SYSTEM - A REVIEW. *Proceedings of the Institute of Electrical and Electronics Engineers*, 56(6), p.1032+.

Räsänen, L., 1981. Adherence of bacteria to human lymphocyte subpopulations and the role of monosaccharides in bacterial binding. *Cellular Immunology*, 58(1), pp.19-28. Available at: http://www.sciencedirect.com/science/article/pii/0008874981901453.

Satomi, T. et al., 2007. Density Control of Poly(ethylene glycol) Layer To Regulate Cellular Attachment. *Langmuir*, 23(12), pp.6698-6703.

Sauerbrey, G., 1959. *Sauerbrey Theory*,

Schild, H.G., 1992. Poly(N-isopropylacrylamide): experiment, theory and application. *Progress in Polymer Science*, 17(2), pp.163-249. Available at: http://www.sciencedirect.com/science/article/pii/007967009290023R.

SchmaljIohann, D., 2006. Thermo- and pH-responsive polymers in drug delivery. *Advanced drug delivery reviews*, 58(15), pp.1655-70.

Schultz, S.G. & Solomon, A.K., 1961. Determination of the Effective Hydrodynamic Radii of Small Molecules by Viscometry. *The Journal of General Physiology*, 44(6), pp.1189-1199.

Schwan, H.P. & Ferris, C.D., 1968. 4-ELECTRODE NULL TECHNIQUES FOR IMPEDANCE MEASUREMENT WITH HIGH RESOLUTION. *Review of Scientific Instruments*, 39(4), pp.481-&

Shain, W., 2012. Complex impedance spectroscopy.

Shortreed, M., Bakker, E. & Kopelman, R., 1996. Miniature Sodium-Selective Ion-Exchange Optode with Fluorescent pH Chromoionophores and Tunable Dynamic Range. *Analytical Chemistry*, 68(15), pp.2656-2662.

Shoval, A. et al., 2009. Carbon nanotube electrodes for effective interfacing with retinal tissue. *Frontiers in neuroengineering*, 2(April), p.4.

Siow, K.S. et al., 2006. Plasma Methods for the Generation of Chemically Reactive Surfaces for Biomolecule Immobilization and Cell Colonization - A Review. *Plasma Processes and Polymers*, 3(6-7), pp.392-418.

Sirringhaus, H. et al., 2000. High-Resolution Inkjet Printing of All-Polymer Transistor Circuits . *Science* , 290 (5499), pp.2123-2126. Available at: http://www.sciencemag.org/content/290/5499/2123.abstract.

Slocik, J.M. et al., 2006. Site-Specific Patterning of Biomolecules and Quantum Dots on Functionalized Surfaces Generated by Plasma-Enhanced Chemical Vapor Deposition. *Advanced Materials*, 18(16), pp.2095-2100.

Slowing, I.I. et al., 2007. Mesoporous Silica Nanoparticles for Drug Delivery and Biosensing Applications. *Advanced Functional Materials*, 17(8), pp.1225-1236.

Song, H.K. et al., 2000. The effect of pore size distribution on the frequency dispersion of porous electrodes. *Electrochimica Acta*, 45(14), pp.2241-2257.

Song, W. et al., 2007. Controllable water permeation on a poly(N-isopropylacrylamide)-modified nanostructured copper mesh film. *Langmuir : the ACS journal of surfaces and colloids*, 23(1), pp.327-31.

Spohr, R. et al., 1998. Thermal control of drug release by a responsive ion track membrane observed by radio tracer flow dialysis. *Journal of Controlled Release*, 50(1–3), pp.1-11.

Standford Research Systems, 2004. Quartz Crystal Microbalance Theory and Calibration The QCM oscillator. , 9040(408).

Stevens, M.M. & George, J.H., 2005. Exploring and Engineering the Cell Surface Interface. *Science*, 310(5751), pp.1135-1138.

Stuart, M.A.C. et al., 2010. Emerging applications of stimuli-responsive polymer materials. *Nat Mater*, 9(2), pp.101-113.

Sun, T. et al., 2004. Reversible Switching between Superhydrophilicity and Superhydrophobicity. *Angewandte Chemie International Edition*, 43(3), pp.357-360.

Suselbeck, T. et al., 2005. In vivo intravascular electric impedance spectroscopy using a new catheter with integrated microelectrodes. *Basic Research in Cardiology*, 100(1), pp.28-34.

Tanaka, M. et al., 2001. Study of Blood Compatibility with Poly(2-methoxyethyl acrylate). Relationship between Water Structure and Platelet Compatibility in Poly(2-methoxyethylacrylate-co-2-hydroxyethylmethacrylate). *Biomacromolecules*, 3(1), pp.36-41.

Tenhaeff, W.E. & Gleason, K.K., 2008. Initiated and Oxidative Chemical Vapor Deposition of Polymeric Thin Films: iCVD and oCVD. *Advanced Functional Materials*, 18(7), pp.979-992.

Tian, H.Y. et al., 2011. Synthesis of Thermo-Responsive Polymers With Both Tunable UCST and LCST. *Macromolecular Rapid Communications*, 32(8), pp.660-664.

Tokarev, I. & Minko, S., 2009. Multiresponsive, Hierarchically Structured Membranes: New, Challenging, Biomimetic Materials for Biosensors, Controlled Release, Biochemical Gates, and Nanoreactors. *Advanced Materials*, 21(2), pp.241-247.

Tsai, Y.C., Li, S.C. & Chen, J.M., 2005. Cast thin film biosensor design based on a Nafion backbone, a multiwalled carbon nanotube conduit, and a glucose oxidase function. *Langmuir the ACS journal of surfaces and colloids*, 21(8), pp.3653-8.

Urban, M., 2011. *Handbook of Stimuli-Responsive Materials*, WILEY-VCH Verlag.

Vaeth, K.M. et al., 2000. Use of Microcontact Printing for Generating Selectively Grown Films of Poly(p-phenylene vinylene) and Parylenes Prepared by Chemical Vapor Deposition. *Langmuir*, 16(22), pp.8495-8500.

Vasilopoulou, M. et al., 2004. Evaluation of poly(hydroxyethyl methacrylate) imaging chemistries for micropatterning applications. *Journal of Materials Chemistry*, 14(22).

Vollmer, F. et al., 2002. Protein detection by optical shift of a resonant microcavity. *Applied Physics Letters*, 80(21), pp.4057-4059.

Vuong, C. & Otto, M., 2002. Staphylococcus epidermidis infections. *Microbes and Infection*, 4(4), pp.481-489.

Waku, T. et al., 2007. PEG Brush Peptide Nanospheres with Stealth Properties and Chemical Functionality. *Macromolecules*, 40(17), pp.6385-6392.

Werner, C. et al., 1999. Insights on structural variations of protein adsorption layers on hydrophobic fluorohydrocarbon polymers gained by spectroscopic ellipsometry (part I). *Colloids and Surfaces A: Physicochemical and Engineering Aspects*, 156(1–3), pp.3-17.

Wisniewski, N. & Reichert, M., 2000. Methods for reducing biosensor membrane biofouling. *Colloids and Surfaces B: Biointerfaces*, 18(3–4), pp.197-219.

Yammine, P. et al., 2005. Surface Modification of Silicone Intraocular Implants To Inhibit Cell Proliferation. *Biomacromolecules*, 6(5), pp.2630-2637.

Yu, T. et al., 2005. Functional Hydrogel Surfaces: Binding Kinesin-Based Molecular Motor Proteins to Selected Patterned Sites. *Advanced Functional Materials*, 15(8), pp.1303-1309.

Yuan, Y. et al., 2004. Polyurethane vascular catheter surface grafted with zwitterionic sulfobetaine monomer activated by ozone. *Colloids and Surfaces B: Biointerfaces*, 35(1), pp.1-5.

Zareie, H.M. et al., 2000. Investigation of a stimuli-responsive copolymer by atomic force microscopy. *Polymer*, 41(18), pp.6723-6727.

Zhang, X.Z. et al., 2002. A novel thermo-responsive drug delivery system with positive controlled release. *International Journal of Pharmaceutics*, 235(1–2), pp.43-50.

Zhou, H. et al., 2005. Glucose biosensor based on platinum microparticles dispersed in nano-fibrous polyaniline. *Biosensors and Bioelectronics*, 20(7), pp.1305-1311.

Zoppe, J.O., Venditti, R.A. & Rojas, O.J., 2012. Pickering emulsions stabilized by cellulose nanocrystals grafted with thermo-responsive polymer brushes. *Journal of colloid and interface science*, 369(1), pp.202-9.

Zubaidi & Hirotsu, T., 1996. Graft polymerization of hydrophilic monomers onto textile fibers treated by glow discharge plasma. *Journal of Applied Polymer Science*, 61(9), pp.1579-1584.